

Genome-wide identification of 12 amino acid transporter families and molecular characterization of their transcriptional responses to various nutrient stresses in allotetraploid rapeseed

Xiao-cai Kong

Zhengzhou University

Cai-peng Yue#

Zhengzhou University

Tian-yu Zhang

Zhengzhou University

Ting Zhou

Zhengzhou University

Jin-yong Huang

Zhengzhou University

Ying-peng Hua (✉ yingpenghua@zzu.edu.cn)

Zhengzhou University

Research Article

Keywords: Brassica napus, amino acid transporters, genome-wide analysis, nutrient stresses

Posted Date: March 24th, 2022

DOI: <https://doi.org/10.21203/rs.3.rs-1435140/v1>

License: © ⓘ This work is licensed under a Creative Commons Attribution 4.0 International License. [Read Full License](#)

Abstract

Background: *Brassica napus* is an important oil crop in China and has a great demand for nitrogen. Amino acid transporters (AAT) play a key role in amino acid absorption and transport in plants. However, the AAT family genes have not been reported in *Brassica napus* so far.

Results: In this study, genome-wide analysis identified 203 AAT members in *Brassica napus* genome. Based on phylogenetic and synteny analysis, BnaAATs were classified into twelve groups. The members in the same subgroups showed that similar physiochemical characteristics, intron/exon and motif patterns. By evaluating *cis*-acting regulatory elements (CREs) in the promoters, we identified some *cis*-acting regulatory elements (CREs) related to hormone, stresses and plant development. Darwin's evolutionary analysis indicated that *BnaAATs* might have experienced strong purifying selection pressure. The *BnaAAT* gene family in *Brassica napus* may have undergone gene expansion, the chromosomal location of *BnaAATs* indicated that whole genome replication or segmental replication may play a major driving role. Differential expression pattern of *BnaAATs* under nitrate limitation, phosphate shortage, potassium shortage, boron stress, boron toxicity, cadmium toxicity, ammonium excess, and salt stress conditions indicated that they were responsive to different nutrient stresses.

Conclusions: In summary, these findings provide a comprehensive survey of the *BnaAAT* genes family and lay a foundation for the further functional analysis of family members. Transcriptome analysis identified genes that responded to stresses, which laid a foundation for the genetic improvement in rapeseed nutrient stress resistance.

Introduction

Nitrogen is an essential element for plant growth and development. Large quantities of nitrogen are required to ensure crop yields [1]. Amino acids are not only a nitrogen source that can be directly absorbed by plants, but also the major transport form of organic nitrogen in plants [2]. Amino acid transporters play an essential role in the transport of amino acids. Amino acid transporters can be divided into two main families, the amino acid transporter (ATF) family and the amino acid-polyamine-choline transporter (APC) family [3]. The ATF family consists of six subfamilies: Amino acid permease (AAP), lysine and histidine-transporter (LHT), proline transporter (ProT), γ -aminobutyric acid transporter (GAT), auxin transporter (AUX) and aromatic and neutral amino acid transporter (ANT). The APC family consists of three subfamilies: cationic amino acid transporters (CAT), amino acid/choline transporters (ACTs) and polyamine H⁺ cotransporters (PHS) [3]. Genes in AAP family have been studied in Arabidopsis. The AAP family contains eight protein members (AtAAP1–8), transporters encoded by AAP family have a variety of functions in plant development and physiology [4]. For instance, *AtAAP1* was highly expressed in cauline and senescent leaves and played an important role in the efficient use of nitrogen sources present in the rhizosphere [5, 6]. Genes in CAT family have also been well studied in Arabidopsis. The CAT family contains nine protein members (AtCAT1–9) and plays a key role in amino acid transport and nitrogen metabolism in plants [7]. For example, *AtCAT2* was primarily localized at the tonoplast and played an important role in maintaining total amino acid levels by exporting amino acids from vacuoles [8]. *AtCAT3* and *AtCAT4* play roles in intracellular compartmentalization of amino acids, intercellular transport through plasmodesmata, and loading/unloading of vascular tissue, respectively [9].

The allotetraploid *Brassica napus* ($AnAnCnCn$, $2n = 4x = 38$) originates from spontaneous hybridization of the diploid *Brassica rapa* ($ArAr$, $2n = 2x = 20$) and *Brassica oleracea* ($CoCo$, $2n = 2x = 18$) [10]. Rapeseed is the most important oil crop in China, and its sown area and output are the first in the world, its yield and quality were greatly affected by N element. Due to the low nitrogen use efficiency of rapeseed, a large amount of nitrogen fertilizer should be invested to ensure the yield of rapeseed [11]. Therefore, improving the N remobilization efficiency in oilseed rapes is important for NUE enhancement through molecular modulation of amino acid transporters.

However, few systematic analyses of AATs in *B. napus* have been identified. Therefore, it is of great significance to excavate *B. napus* AAT members of analyzing the nutritional physiological and biological characteristics of rapeseed. In this study, we were aimed to identify the genome-wide AAT genes in *B. napus*, characterize the genomic characteristics and transcriptional responses of the AATs to N stresses, including nitrate limitation and ammonium toxicity, and investigate the transcriptional responses of AATs to other nutrient stresses, including phosphate limitation, boron limitation, boron toxicity, potassium deficiency, cadmium toxicity, and salt stress. The method of bioinformatics and molecular biology was used to identify to compare and analyze the expression of *B. napus* AATs. Through the statistics of the transmembrane region of BnaAAT proteins, the prediction of the active site, the phylogenetic analysis, the *cis*-acting regulatory elements (CREs) analysis, the protein interaction and the expression pattern exploration, it can provide partial reference for the related studies of amino acid transporter and nitrogen nutrient metabolism in rapeseed.

Results

Identification of BnaAAT genes

According to the protein sequences of AAT family in *Arabidopsis*, 203 BnaAAT members were identified in the *B. napus* genome. Besides, we used amino acid sequences of AAT family members in *A. thaliana* as query conditions, screened and identified the homologs of *B. oleracea* and *B. rapa* in BRAD database through PFAM (PF01490 and PF00324) domain. As shown in (Table 1), AATs had 63 members in the model *A. thaliana* and each AAT member only had a single copy. A total of 105, 107, and 203 AAT homologs were identified in *B. rapa*, *B. oleracea*, and *B. napus*, respectively. The results showed that the homolog number of AATs in *B. napus* was similar to the sum of AATs in both *B. rapa* and *B. oleracea* (Table 1). Indicating that most AATs was kept during the spontaneous hybridization between *B. rapa* and *B. oleracea* for the formation of allotetraploid *B. napus*. However, we found that *ATLb5s*, *LHT3s*, *ProT3s*, and *CAT7s* were lost in *B. napus* (Additional file 1: Table S1). The changes in the BnaAAT number might indicate their critical differential roles in the resistance of *B. napus* to N stresses.

Chromosomal Distribution and Duplication Analysis of BnaAATs

Gene expansion occurs during the evolution of species [6]. To identify the expansion patterns of *AAT* genes in Brassicaceae species, we investigated their segment duplication in duplicated blocks within each subfamily. We totally identified 257 pairs of *AATs* within 12 subfamilies, including 30 pairs of *BnaAAPs*, 8 pairs of *BnaANTs*, 35 pairs of *BnaATLAs*, 42 pairs of *BnaATLbs*, 22 pairs of *BnaAUXs*, 5 pairs of *BnaGATs*, 41 pairs of *BnaLHTs*, 40 pairs of *BnaProTs*, 2 pairs of *BnaTTPs*, 4 pairs of *BnaACTs*, 18 pairs of *BnaCATs*, and 10 pairs of *BnaLATs* (Fig. 1). The *BnaAAT* genes were unevenly distributed in different chromosomes (Additional file 1: Figure S1). The chromosomes C04, Cnn_random and A09 had more *BnaAATs*, including 14 *BnaAATs*, respectively. While chromosome A05 possessed 13 *BnaAATs* (Additional file 1: Figure S1). Moreover, 12 genes are located on chromosome C03; 11 genes are located on chromosome C08; 10 genes each are located on chromosome A04, A03 and C02; 9 genes each are located on chromosome Ann_random, A02 and C06; 8 genes are located on chromosome A07; 6 genes each are located on chromosome C09, A03_random, C05, C07 and A08; 5 genes each are located on chromosome A10 and A06; 4 genes are located on chromosome A09_random; 3 genes are located on chromosome A06_random; 2 genes each are located on chromosome C05_random, C01 and A01; 1 gene each are located on chromosome A04_random, C07_random, A05_random, C01_random, C06_random, Unn_random and C03_random (Additional file 1: Figure S1). Gene family expansion occurs mainly through four pathways: tandem replication, fragment replication, whole genome replication (polyploidy) and replication transposition [12]. Gene duplication plays a key role in plant evolution. Comparative genomics revealed that the *Arabidopsis* genome can be divided into 24 ancestral cruciferous blocks labeled as A-X [13]. The results showed that *AAT* family members in *Arabidopsis* and their corresponding homologues in *B. napus* were located in the same chromosomal segment (Additional file 1: Table S1). According to the genomic distribution of *BnaAATs*, we found that whole-genome duplication and segmental duplication are the main ways of *BnaAATs* expansion, except *BnaA9.AAP8a*, *BnaA9.AAP8b*, *BnaC8.AAP8a*, *BnaC8.AAP8b*, *BnaC8.AAP8c*, *BnaC4.ProT1a*, *BnaC4.ProT1b*, *BnaC2.NHX1a* and *BnaC2.NHX1b*, *BnaA6.AAP8a*, *BnaA6.AAP8b*, *BnaA3.ATLb8a*, *BnaA3.ATLb8b*, *BnaA9.ATLa2a*, *BnaA9.ATLa2b*, *BnaA9.ATLa2c*, *BnaA3.AUX1a* and *BnaA3.AUX1b*, which were derived from tandem duplication (Additional file 1: Figure S1).

Phylogeny analysis of *BnaAATs*

To analyze the evolutionary relationship of *BnaAAT* proteins, 12 unrooted phylogenetic tree was constructed using MEGA 10.2.2 (Fig. 3). Sequences from the same homolog were all clustered together (Fig. 3). Besides, we conducted a detailed analysis of the CAT subfamily. Based on a previous study, *Arabidopsis* CAT proteins were divided into three clades. To analyze the evolutionary relationship of *B. napus* CAT proteins, a neighbor-joining phylogenetic tree was constructed by comparing *B. napus* CAT amino acid sequences with CATs from three other plant species, including dicotyledonous plants (*Arabidopsis*) and two monocotyledonous plants (wheat and rice). The results showed that Group I contained 29 CAT members, including AtCAT1/5/8 and BnaCAT1/5/8 (Fig. 2). Group II contained 14 CAT members, including AtCAT6/7 and BnaCAT6 (Fig. 2). Group III contained 24 CAT members, including AtCAT2/3/4 and BnaCAT2/3/4 (Fig. 2). Group IV contained 6 CAT members, including AtCAT9 and BnaCAT9 (Fig. 2). Both dicotyledonous and monocotyledonous members existing in every clade indicated that gene expansion of the CAT family members occurred before the ancestral divergence of monocotyledons and dicotyledons.

Molecular characterization of *BnaAATs*

To understand the molecular characteristics of the *BnaAATs*, we calculated the physicochemical parameters of each *BnaAAT* using ExPASy. The results indicated that most proteins in the same *AAT* subfamily had parallel parameters (Additional file 1: Table S1). In summary, the coding sequence (CDS) lengths of *BnaAATs* varied from 981 bp (*BnaA4.ATLa4*) to 1551bp (*BnaA6.BAT1a*), corresponding to the variation of the deduced amino acid number from 326 bp (*BnaA4.ATLa4*) to 679 bp (*BnaA6.BAT1a*) (Additional file 1: Table S1). The computed molecular weights of *BnaAATs* ranged from 35.89 KD (*BnaA4.ATLa4*) to 75.1 KD (*BnaA6.BAT1a*) (Additional file 1: Table S1). The theoretical isoelectric points (pIs) of *BnaAATs* varied from 4.79 (*BnaC3.ATLb3*) to 9.61 (*BnaA2.ATLb10a*), with some of them > 7.0 and some of them < 7.0 (Additional file 1: Table S1). The GRAVY index reflects the hydrophilic and hydrophobic nature of the protein physicochemical properties. The results indicated that the GRAVY values of the *BnaAAT* members ranged from 0.247 (*BnaC4.ATLb4b*) to 0.891 (*BnaA3.ANT4*) (Additional file 1: Table S1). As a result, all the *AAT* proteins in *B. napus* were thought to be hydrophobic. Most instability indices of *BnaAATs* were < 40.0 (Additional file 1: Table S1), and it indicated that most *BnaAATs* showed strong protein stability. And the online WoLF PSORT was used to predict the subcellular localization of 203 *BnaAATs* (Additional file 1: Table S1). The results indicated that most of them were localized in the plasma membrane, suggesting that they might account for the trans-membrane transport of amino acid. We utilized the TMHMM Server v2.0 (<http://www.cbs.dtu.dk/services/TMHMM/>) to predict the transmembrane structures of *AATs* in *A. thaliana* and *B. napus*. We found that the number of TM regions in most *BnaAATs* ranges from eight to twelve (Additional file 1: Table S1), and *BnaAATs* of the same family have similar number of TM regions. For example, 10 TMs in AUX, 13 TMs in ACT and 11 TMs in ATLa. These findings indicated that *AATs* of the same subfamily were quite conservative in structure.

Identification of evolutionary selection pressure on *BnaAATs*.

To characterize selection pressure on the *BnaAATs* during the evolutionary process, we used the orthologous *AAT* pairs between *B. napus* and *A. thaliana* to calculate the values of synonymous (K_s) and nonsynonymous (K_a) nucleotide substitution rates, and K_a/K_s (Additional file 1: Table S1). The K_a values of *BnaAATs* ranged from 0.01404 (*BnaC6.AUX4*) to 0.42935 (*BnaC7.CAT6*) with an average of 0.0676, and the K_s values of *BnaAATs* ranged from 0.2216 (*BnaC8.AAP8a*) to 2.1475 (*BnaC7.CAT6*), with an average of 0.5114 (Additional file 1: Table S1). Further, we found that all the K_a/K_s values of *BnaAATs* were < 1.0 (Additional file 1: Table S1). Therefore, we predicted that *BnaAATs* might have undergone a very strong negative selection pressure to preserve their function. The K_s values of duplicated homologs among gene families are usually thought to be molecular clocks, and they are presumed to be unaltered over time. The segregation between the model *Arabidopsis* and its derived *Brassica* species occurred 12–20 million years ago (Mya) [12]. Our results indicated that most *BnaAATs* might diverge from *AtAATs* approximately 11.0–20.0 Mya (Additional file 1: Table S1), which indicated that the *Brassica* plant speciation might be accompanied by the *AAT* divergence.

Conserved motifs, gene structure analysis of *BnaAATs*

The 203 putative BnaAAT protein sequences contained a typical Aa trans domain through the Pfam analysis. 15 conserved motifs in *B. napus* were extracted by the MEME program based on protein sequences. The results showed that several motifs were widespread among BnaAATs, such as motif 1, 2, 5, 7, and thus might be used as the indicators of the AAP family members (Fig. 3). The figure has shown that the BnaAATs in the same subgroups have similar distributions of motifs, while there were some differences in the different subgroups. The comparison indicated that some *BnaAAT* genes in the same subgroups are likely to have similar functions.

Furthermore, an exon-intron diagram was constructed based on the corresponding coding and genome sequences (Fig. 3). The results showed that the same group shared similar exon/intron structures, such as *BnaA7.AAP3* and *BnaC6.AAP3b*, *BnaA6.BAT1b* and *BnaC7.BAT1*, *BnaA7.AUX4* and *BnaC6.AUX4*, *BnaA3.LHT7* and *BnaC7.LHT7*. On the contrary, some *BnaAATs* in the same cluster also showed differences in intron/exon organization. Significant variations were found in the 5'-UTR or/and 3'-UTR of some genes as compared with their paralogy, such as *BnaA6.BAT1a*, *BnaA9.ATLb4*, *BnaA3.AUX3*, *BnaCn.LAT3*, et al (Fig. 3). The introns of thirteen *BnaAAT* genes are absent from the open reading frames, and the number of introns in other coding sequences ranged from one to thirteen (Fig. 3). These results indicated that members of a group had a similar intron/exon pattern, corresponding to the clusters of *BnaAATs*. Studies on the conserved motif composition, gene structure and phylogenetic relationship have demonstrated that BnaAATs have very conserved amino acid residues, and members of the group may have similar functions.

Cis-acting regulatory elements (CREs) analysis of the promoter regions of the BnaAAT genes

Cis-acting regulatory elements (CREs) play a key role in the regulation of gene expression. To explore gene function and regulation patterns, 2000bp sequence of *BnaAAT* genes was submitted to PlantCare database. The *cis*-acting regulatory elements (CREs) of the *BnaAAT* genes mainly classified into three categories: plant growth and development, stress responsive elements and phytohormone responsive elements. In the first category the elements mainly include meristem expression (CAT-box), light responsiveness (Box 4) zein metabolism regulation (O2-site), endosperm expression (GCN4-motif), seed-specific regulation (RY-element), cell cycle regulation (MSA-like), circadian control (circadian), differentiation of the palisade mesophyll cells (HD-Zip 1) and flavonoid biosynthetic gene regulation (MBSI) (Additional file 1: Figure S3). In the second category (stress-responsive), the elements included wound-responsive (WUN motif), anaerobic induction (ARE), low-temperature-responsive (LTR) and MYB-binding sites involved in drought inducibility (MBS), anoxic specific inducibility (GC-motif) and stress responsiveness (TC-rich repeats) (Additional file 1: Figure S3). In the third category (phytohormone responsive), the elements included gibberellin responsiveness (P-box), methyl jasmonate-responsive (CGTCA-motif), MeJA-responsiveness (TGACG-motif), gibberellin-responsive element (GARE-motif), auxin-responsive (TGA-element), salicylic acid responsiveness (TCA-element), and abscisic acid-responsive (ABRE) (Additional file 1: Figure S3). Among these *cis*-acting regulatory elements (CREs), ABRE, ARE and CGTCA-motif were conspicuous, which were involved in abscisic acid responsiveness, anaerobic induction and MeJA-responsiveness (Additional file 1: Figure S3). These results indicated that *BnaAAT* genes may be able to be induced or repressed by abiotic stress and subsequently participate in plant stress resistance. Interestingly, each of *BnaAAT* gene possessed different kinds and number of *cis*-acting regulatory elements (CREs), we can speculate that under different growing and development status, environmental conditions, *BnaAAT* genes might function independently or synergistically to guarantee plant growth and development normally.

Protein-protein interaction analysis of BnaAATs

To further identify the protein(s) potentially interacting with the AAT family members, we constructed a protein interaction networks of AATs using the STRING database. As shown in figure, the proteins closely related to CAT proteins in *Arabidopsis thaliana* are mainly polyamine absorption transporter PUT (polyamine uptake transporter) and some amino acid permeability enzymes AAP (amino acid permease) (Additional file 1: Figure S7). Amino acid permeases (AAPs) are involved in transporting a broad spectrum of amino acids and regulating physiological processes in plants [14]. In the ANT and BAT subfamily, except ANT1, the other ANTs and BATs also interacted with AAP (Fig. 4, Additional file 1: Figure S4), which serves a job-sharing improves AA transport from sources to sinks and further enhances plant N use efficiency (NUE) [15]. In the AUX subfamily, all the AUXs interacted with PIN (Fig. 4), which belongs to auxin efflux carrier family protein. In the ProT subfamily, all the ProTs consistently interacted with BON (Additional file 1: Figure S4), which is a member of a newly identified class of calcium-dependent, phospholipid binding proteins. In the LHT subfamily, PHS subfamily and AAP subfamily, LHT1, LHT2, LHT6, all the LATs and all the AAPs were consistently interacted with CAT (Additional file 1: Figure S5, S8, S9), cation AA transporters (CATs) belonging to the APC family [16]. Besides, some other proteins such as TOR (Serine/threonine-protein kinase), NRT 1.7 (Low-affinity proton-dependent nitrate transporter), SNF4 (Homolog of yeast sucrose nonfermenting 4), SIAR1 (Silique Are Red 1), and the UMAMIT (Usually Multiple Acids Move In and out Transporters) family members, VDAC3 (Mitochondrial outer membrane protein porin 3) and PP2CG1 (Protein phosphatase 2C family protein) were also found to interact with the AAT proteins (Additional file 1: Figure S4-S9).

Expression Analysis of BnaAAT Genes in Various Tissues

To identify the expression patterns of *BnaAAT* genes, the tissue-specific expression pattern of *BnaAATs* was analyzed in various tissues including blossomy pistil, bud, ovule, leaf, wilting pistil, pericarp, root, sepal, silique, stamen, and stem (Fig. 5). Results indicated that *BnaAAT* genes were constitutively expressed among several tissues, but some genes presented preferential expression in particular tissues. For instance, *BnaAAP2s/ BnaAAP3s/ BnaA9.AAP8a/ BnaA9.AAP8b/ BnaA4.CAT5/ BnaC8.CAT8/ BnaA9.ProT2/ BnaC6.ATLa5a/ BnaA7.ATLa5b/ BnaC9.LHT1/ BnaC2.ATLb10/ E* were preferentially expressed in roots; *BnaA4.ProT1/ BnaA2.TTP2* in blossomy pistil; *BnaA8.CAT1/ BnaC3.CAT1/ BnaLHT8s/ BnaLHT2s/ BnaC4.ATLb3/ BnaA5.ATLb3/ BnaA4.ATLb4/ BnaC3.LAT5/ BnaA3.LAT5* in bud; *BnaA6.AAP8a/ BnaC5.AAP8a/ BnaA3.CAT6/ BnaAn.CAT9/ BnaUn.GAT2/ BnaC3.LHT7/ BnaC3.AUX1/ BnaA3.AUX1b/ BnaC3.ATLb3/ BnaC3.ATLb8/ BnaCn.LAT3/ B* in ovule; *BnaC3.AAP4/ BnaA9.ATLb4/ BnaA5.LAT4/ BnaC2.TTP2* in leaf; *BnaA5.CAT4/ BnaA5.ANT1/ BnaC5.ANT1/ BnaANT4s/ BnaCn.ATLa1/ BnaC4.ATLa4/ BnaA7.ATLa5a/ BnaA3.LHT7/ BnaC7.LHT7/ BnaC1.LHT7/ BnaA6.ATLb1/ Bn* in new pistill; *BnaA7.ATLa4/ BnaC6.AUX4* in pericarp; *BnaAAP2s/ BnaAAP3s/ BnaA9.AAP8s/ BnaC8.AAP8b/ BnaA4.CAT5/ BnaC8.CAT8/ BnaA4.GAT2/ BnaA9.ProT2/ BnaA7.ATLa5b/ BnaC9.LHT1/ BnaCn.AUX4/ BnaC2.ATLb10s/*

in root, *BnaC8.ProT2*, *BnaA4.AUX1* and *BnaA5.AUX1* showed highly expressed in sepal while *BnaA6.AAP8a*, *BnaC5.AAP8a* and *BnaC6.LHT1* was highly concentrated in silique (Fig. 5). In the AUX subfamily, *BnaAUX3s* exhibited highly expressed in stamen, *BnaAUX2s* preferentially expressed in stem. The most genes of CAT subfamily, *ProT* subfamily, *ANT* subfamily *ATLa* subfamily showed highly expressed in wilting pistil, especially *BnaA3.CAT1*, *BnaA9.CAT2b*, *BnaCn.CAT2*, *BnaC5.CAT4* and *BnaC8.ATLa2* (Fig. 5). What's more, six genes showed no expression in any tissues (*BnaA2.LHT5*, *BnaA5.LHT10*, *BnaA9.ATLa2b*, *BnaA3.ATLb6*, *BnaC3.ATLb6*, *BnaA3.ATLb8a*) (Fig. 5).

Transcriptional analysis of *BnaAATs* under diverse nutrient stresses.

Transcriptional identification of the core *AAT* members was very important to the further understanding of the *BnaAATs* function. The high yield of rapeseed depends on the extensive application of nitrogen fertilizer, however N use efficiency is low [17]. When N supplies is insufficient, plants usually to develop a set of adaptive responses to limited N growth conditions [18]. However, the molecular mechanisms underlying the use of nitrogen by plants has not been fully understood [6]. The transcript levels of *BnaAAT* genes after low-N treatment were investigated to better understanding of the role in assimilating N. Under N stress, the expression of 122 *BnaAATs* was significantly altered in the shoots and roots (Fig. 6). In the shoots, the expression of 92.6% (113 *BnaAATs*) was up-regulated, but 17% (21 *BnaAATs*) were down-regulated (Fig. 6). Besides, the expression levels of 9 *BnaAATs* did not change. In the roots, 118 *BnaAATs* responded to N stress, the expression of 64.4% (76 *BnaAATs*) was significantly induced, while 33.8% (40 *BnaAATs*) were suppressed (Fig. 6). In this work, we found that most of the *BnaAAT* family genes were up-regulated in the shoots or roots under the condition of N limitation (Fig. 6).

Phosphorus (P) is one of the essential nutrient elements for crop growth, and occupies an irreplaceable position in agricultural production [19]. Under phosphate limitation condition, a total of 72 DEGs were identified in the shoots and roots (Fig. 7). In the shoots, no different expression of eight *BnaAATs* (*BnaC4.LHT6*, *BnaC6.LHT1*, *BnaA4.ATLb4*, *BnaC6.ATLa5a*, *BnaA6.AAP4*, *BnaC3.AAP4*, *BnaA10.AAP2*, *BnaC7.CAT6*) was observed between sufficient phosphate and insufficient phosphate conditions (Fig. 7). The expression of 43 *BnaAATs* clearly up-regulated in the shoots under the condition of low phosphorus, but the expression of 21 *BnaAATs* was obviously suppressed (Fig. 7). In the roots, under phosphate limitation condition, the expression of 20 *BnaAATs* was distinctly down-regulated, while 40 *BnaAATs* showed higher expression levels (Fig. 7). And the expression of 12 *BnaAATs* was no significant changes between sufficient phosphate and insufficient phosphate conditions (Fig. 7).

Potassium (K) is an important macronutrient in plants [20]. Potassium enhances crop resistance to a variety of biological and abiotic stresses [21, 22]. Under the condition of low potassium treatment, a total of 88 *BnaAAT* DEGs were identified in the shoots or roots (Fig. 8). Under low K treated group, 52.3% (46 *BnaAATs*) were induced in the shoots, especially *BnaC6.LHT1/BnaAn.LHT1/BnaC1.LHT7/BnaAn.LHT7/BnaA4.CAT5*. On the contrary, the expression of 39.8% (35 *BnaAATs*) was significantly decreased (Fig. 8). However, we did not find the differential expression of eight *BnaAATs* (*BnaA6.AAP4*, *BnaC8.AAP8b*, *BnaA9.AAP8a*, *BnaCn.LHT9*, *BnaC8.ProT2*, *BnaA4.ATLb4*, *BnaC4.TTP1*, *BnaC7.CAT6*) between sufficient potassium and insufficient potassium conditions in the shoots (Fig. 8). In the roots, K deficiency resulted in a significantly increase in the expression of 36 *BnaAATs*, while obviously decrease the expression of 45 *BnaAATs*. Besides, the expression of seven *BnaAATs* (*BnaA1.AAP1*, *BnaC4.LHT1*, *BnaA3.ProT1*, *BnaA2.TTP2*, *BnaCn.CAT2*, *BnaA9.CAT8*, *BnaA4.CAT5*) did not change significantly (Fig. 8).

Boron is one of the essential trace elements in plants [23], boron deficiency causes plants to flower unfrugally. Boron toxicity has great influence on root length of plants [23]. However, whether *BnaAATs* function in B-mediated plant growth is unclear. Under the condition of deficient-B and excess-B, differentially expressed *BnaAATs* were identified to evaluate the effects of B on *BnaAAT* gene expression. Under the condition of deficient-B, we identified a total of 69 *BnaAAT* DEGs in the shoots and roots (Fig. 9). In the shoots, the expression of 65 *BnaAATs* was altered. 43 *BnaAATs* were induced by deficient-B, but 21 *BnaAATs* were suppressed by boron deficiency (Fig. 9). In the roots, 50 *BnaAATs* responded to B-deficiency. 21 *BnaAATs* were up-regulated, while 28 *BnaAATs* were down-regulated by B-deficiency. The expression of four *BnaAATs* (*BnaA3.ATLb8b*, *BnaA6.BAT1b*, *BnaC8.AAP8c*, *BnaC4.AAP1*) was unaffected in the shoots, while 19 *BnaAATs* (*BnaA8.LHT4*, *BnaCn.LHT9*, *BnaA9.AUX3*, *BnaCn.AUX2*, *BnaC3.ProT1*, *BnaAn.ATLa3*, *BnaA2.ATLb1*, *BnaC2.ATLb1*, *BnaC3.ATLb3*, *BnaA9.ATLb4*, *BnaC2.BAT1*, *BnaA1.LAT4*, *BnaCn.CAT2*, *BnaA5.CAT4*, *BnaA9.AAP7*, *BnaA9.AAP8a*, *BnaA3.AAP1*, *BnaA7.AAP3*) were unchanged in the roots (Fig. 9). B toxicity also influenced *BnaAATs* expression. We identified a total of 55 *BnaAAT* DEGs in the shoots and roots. In the shoots, 21 *BnaAATs* were induced, but 28 *BnaAATs* were repressed under the condition of B stress. In the roots, only 11 *BnaAATs* were induced, but 33 *BnaAATs* were repressed by B toxicity (Fig. 10). In the shoots, the expression of six *BnaAATs* (*BnaA5.LHT6*, *BnaC8.GAT1*, *BnaA7.ATLa5a*, *BnaA6.BAT1b*, *BnaA9.AAP8b*, *BnaC8.AAP8a*) didn't change, while 11 *BnaAATs* (*BnaAn.LHT7*, *BnaA3.ProT1*, *BnaC3.ProT1*, *BnaA6.ATLb1*, *BnaA9.ATLb4*, *BnaCn.ATLb9*, *BnaC2.BAT1*, *BnaA5.CAT4*, *BnaC6.AAP3b*, *BnaA2.AAP4*, *BnaA7.LHT2*) didn't change under the condition of B toxicity compared with control condition (Fig. 10).

Ammonium is a major inorganic nitrogen source for plants. At low external supplies, ammonium promotes plant growth, while at high external supplies it causes toxicity [24]. Under different forms of nitrogen conditions, we identified a total of 89 *BnaAAT* DEGs in the shoots and roots (Fig. 11). In the shoots, 48 *BnaAATs*, especially *BnaCn.LHT9*, *BnaC9.AAP7*, *BnaAn.CAT5* were up-regulated under the condition of ammonium stress, while the expression of 30 *BnaAATs* was decreased (Fig. 11). And the expression of remained genes (*BnaA5.ProT1a*, *BnaC4.ProT1b*, *BnaCn.AUX2*, *BnaA4.GAT2*, *BnaC8.GAT1*, *BnaC9.ATLa3*, *BnaA9.ATLa3*, *BnaC3.ATLb3*) didn't change obviously. In the roots, a total of 77 *BnaAATs* responded to ammonium stress (Fig. 11). Among the differentially expressed 77 *BnaAATs*, 52 *BnaAATs* were increased by A toxicity, but 40 *BnaAATs* were decreased under the condition of ammonium stress compared with control condition (Fig. 11).

Salt stress will induce the accumulation of misfolded or unfolded proteins in plants to inhibit the normal growth and development of plants [25]. The salt altered the expression of 97 *BnaAATs* in the roots or shoots (Fig. 12). After salt treatment, 53.6% (52 *BnaAATs*) and 46.4% (45 *BnaAATs*) of *BnaAATs* were up-regulated and down-regulated in the shoots, respectively, while 47.4% (46 *BnaAATs*) and 48.4% (47 *BnaAATs*) of *BnaAATs* expression levels were positively and negatively regulated in the roots, respectively (Fig. 12). Besides, the expression levels of four *BnaAATs* (*BnaA7.LHT2*, *BnaA9.LHT2*, *BnaC6.LHT8*, *BnaC7.LHT2*) were not changed (Fig. 12). In a word, these results strongly indicated that most *BnaAATs* play key roles in plants respond to salt stress.

Cadmium (Cd) is known as one of the most hazardous elements in the environment and a persistent soil constraint toxic to all flora and fauna [26]. To better understand the role of rapeseed *AATs* in response to cadmium toxicity, we analyzed their transcriptional expression under cadmium toxicity. Under cadmium toxicity, the expression levels of 85 *BnaAATs* were changed in the shoots or roots. The expression of 38 *BnaAATs* significantly increased in the shoots after cadmium stress treatment, but the expression of 21, especially *BnaA6.AAP4*, *BnaC3.AAP4* and *BnaA7.ATLa5a* was suppressed (Fig. 13). However, the expression of 26 *BnaAATs* didn't change obviously in the shoots (Fig. 13). More *BnaAATs* were influenced by cadmium stress, in the roots. In the roots, the expression of 46 *BnaAATs* was inhibited by cadmium stress, while 29 *BnaAATs*, especially *BnaA9.ATLa2b*, *BnaA9.ATLa2c* and *BnaC8.ATLa2*, presented higher expression levels under cadmium stress (Fig. 13). Besides, we did not identify the differential expression of *BnaAATs* (*BnaC4.ProT1c*, *BnaCn.ATLa*, *BnaA7.ATLa5a*, *BnaA9.ATLb4*, *BnaA6.BAT1a*, *BnaC8.AAP8b*, *BnaC8.AAP8c*, *BnaC9.AAP7*, *BnaAn.AAP5*, *BnaC3.AAP2*) under the condition of cadmium stress, in the roots (Fig. 13).

Discussion

AAT family members have been reported to play an important role in plant growth and development, nutrient metabolism and stress resistance [3]. *AAT* members have also been widely studied in other species. For example, *AATs* had 63 members in the model *A. thaliana*, and each *AAT* member only had a single copy. A total of 85 *AATs* in rice [27], 189 *AATs* in soybean, 283 *AATs* in wheat [28], 72 *AATs* in potato [29]. However, the information about *B. napus AATs* are limited so far. In this study, 203 *AAT* genes were identified in *B. napus*. We used bioinformatics methods to analyze the physical and chemical properties, structure and function of proteins encoded by *BnaAAT* family. Subsequently, we performed analyses of their conserved domain, gene structure, gene phylogeny, promoter, and synteny analyses. Besides we constructed their protein-protein interaction network. Furthermore, differential expression of *BnaAATs* under different nutrient conditions was analyzed. These results might provide an integrated insight into the function of *AAT* family genes.

Synthetic analysis of molecular characteristics of *BnaAATs*

From the analysis on the proteins encoded by *BnaAAT* family, we found that the subcellular localization of proteins encoded by the *BnaAAT* family was mainly in plasma membrane (Additional file 1: Table S1), which might be correlate with their function. Most of proteins encoded by *BnaAAT* genes contain 8–12 transmembrane regions, which may be closely related to the regulation of amino acid absorption and transport by the *BnaAAT* genes (Additional file 1: Table S1, Figure S2) [30]. According to phylogenetic analysis, orthologous gene pairs associated with *BnaCATs* were showed to have existed before the ancestral divergence of dicotyledonous and monocotyledonous plants (Fig. 2) [31]. Motifs of *BnaAAT* genes clustered in the same clade were very close, including the number and type (Fig. 3). However, different subgroups contained different conserved motifs. Therefore, we speculated that different types of unique motifs may be the main cause of *BnaAAT* genes functional differentiation [32].

Homolog number variations of *AATs* in allotetraploid rapeseed indicated their functional divergence.

In the present study, a total of 203 *BnaAAT* genes were identified in the rapeseed genome (Table 1). The collinearity results showed that there were a large number of collinearity relationships among *BnaAAT* genes and genome-wide replication events/fragment replication may be the main cause of *BnaAAT* gene family amplification (Fig. 1). Comparative genomics studies have shown that brassica species, such as *B. rapa* and *B. oleracea*, experienced triploidy at the genomic level about 20 million years ago [33, 34]. As a result, there are three copies of each *Arabidopsis* gene in *B. rapa* and *B. oleracea*. 63 *AAT* genes were identified in *Arabidopsis* genome (Table 1). Theoretically, 189 *AAT* genes should be identified in *B. rapa* and *B. oleracea* after complete genome replication, but only 107 genes were found in *B. oleracea* genome (Table 1). *B. napus* originates from spontaneous hybridization of the diploid *B. rapa* ($ArAr$, $2n = 2x = 20$) and *B. oleracea* ($CoCo$, $2n = 2x = 18$) [[10, 35]. Therefore, there should be six homologous genes for each *Arabidopsis* gene in *Brassica napus*. Unlike conventional theory, only 203 *BnaAAT* genes were identified in this study, indicated that some *AAT* genes were lost after whole genome replication. Therefore, we speculated that *AATs* underwent strong selection during the evolution of *B. napus*, and the retained *AAT* gene should have an important function in *B. napus*. Most of the *AtAATs* in *B. napus* had more than one and less than six direct homologous genes, suggested that the *AAT* gene family has expanded but contracted during the diversification of *Brassica napus*. In addition, the homologous genes of *AtVAAT7*, *AtLHT3*, *AtProT3* and *AtCAT7* were not found in the genome of *Brassica napus* (Additional file 1: Table S1). The lost *AATs* may be redundant genes that are gradually replaced by other genes with similar functions [36, 37]. This work also revealed that all *AAT* genes in *Brassica napus* may have undergone rigorous purification selection, which plays a key role in maintaining gene numbers.

Transcriptional analysis of *BnaAATs* under diverse nutrient stresses.

To better understand the potential biological functions of *BnaAATs* in the growth and development of *B. napus*. The expression patterns of *BnaAATs* were analyzed in different tissues, including blossomy pistil, bud, ovule, leaf, wilting pistil, pericarp, root, sepal, silique, stamen, and stem (Fig. 5). Most of the *B. napus* grain nitrogen originates from senescing leaves [11] and are transported through phloem transport. As a result, phloem loading and transport of amino acids is particularly important to seed yield and quality. It has been reported that *AtAAP8* was mainly expressed in the phloem of the source leaf and located on the plasma membrane of the cell. It mainly involved in amino acid loading in phloem and nitrogen distribution in source-sink and then affect the growth of source leaf and seed yield [38]. *PtCAT11* was mainly expressed in phloem and played an important role in amino acid transport between "sourcing" and "sink" tissues during leaf senescence [39]. Here, we found that *BnaC3.AAP4*, *BnaA9.ATLb4*, *BnaA5.LAT4* and *BnaC2.TTP2* were highly expressed in leaves (Fig. 5). Therefore, we speculated that these genes might be responsible for transport of removable amino acids from source tissues to sink grains for protein synthesis after anthesis. It has been reported that *AtAAP1*, *AtAAP5* and *AtLHT1* in *Arabidopsis* play an important role in acquisition of the neutral and cationic amino acids from the soil, respectively [40]. We found that *BnaAAP2s*, *BnaAAP3s*, *BnaA9.AAP8s*, *BnaC8.AAP8b*, *BnaA4.CAT5*, *BnaC8.CAT8*, *BnaA4.GAT2*, *BnaA9.ProT2*, *BnaA7.ATLa5b*, *BnaC9.LHT1*, *BnaCn.AUX4*, *BnaC2.ATLb10s*, *BnaA6.BAT1b*, *BnaC7.BAT1* and *BnaLAT1s* were predominantly expressed in the roots (Fig. 5), suggesting that they might play important roles in root uptake of individual amino acids for *B. napus* growth at different developmental stages. In order to determine the role of *BnaAAT* genes in various stresses, the expression patterns of *BnaAAT* genes were studied. In this work, we found that most of the *BnaAAT* family genes were upregulated in the shoots and roots under the condition of N limitation. It has been reported in apple that *CATs* were up-

regulated with the times of nitrogen starvation treatment, and reached the maximum value at 12 h of treatment [7]. It has been reported that AtAAP1 played important role in efficient use of nitrogen sources present in the rhizosphere [5]. At low nitrogen levels, *BnaC8.AAP8a*, *BnaA6.AAP8a*, *BnaA6.AAP8b*, *BnaA4.ATLa4*, *BnaC7.ATLb1*, *BnaA6.ATLb1*, *BnaA3.CAT1*, *BnaA4.AUX1*, *BnaA8.LHT9*, *BnaAn.LHT1*, *BnaAn.LHT7*, *BnaA9.LHT9*, *BnaA4.ProT2*, *BnaC4.TTP1*, *BnaA6.BAT1b*, *BnaA2.BAT1*, *BnaC7.BAT1*, *BnaA4.GAT2* and *BnaA8.GAT1* were significantly induced in the shoots (Fig. 6). *BnaC2.AAP4*, *BnaA9.AAP7*, *BnaA8.AAP5*, *BnaA2.AAP4*, *BnaAn.ATLa3*, *BnaC2.ATLb1*, *BnaA5.CAT4*, *BnaAn.CAT5*, *BnaA4.CAT5*, *BnaC8.AUX3*, *BnaA9.AUX3*, *BnaA4.ProT1*, *BnaC4.ProT1c*, *BnaC5.LAT4*, *BnaA5.LAT4*, *BnaCn.LAT3*, *BnaA2.TTP2*, *BnaC2.TTP2* and *BnaC3.ANT1* were obviously up-regulated in the shoots under low nitrogen treatment (Fig. 6). We speculated that the enhanced expression of *BnaAATs* contribute to the absorption of amino acids from source to reservoir. Ammonium toxicity causes inhibition of root and shoot growth, it has been reported that a plant's tolerance to ammonium is related to its capacity for ammonium assimilation [41]. Once ammonium entered plant cells, ammonium is rapidly assimilated into glutamine and glutamate via the glutamine synthetase-glutamate synthase (GS-GOGAT) cycle [42]. In this work, we identified that the expressions of some *BnaAATs* were changed in response to ammonium toxicity (Fig. 11), which indicated their potential function in the alleviation of excessive ammonium-caused damages to rapeseed. In this work, we found that most *BnaAAT* DEGs were induced in the shoots or roots under the condition of phosphate limitation. It indicated that the phosphorus deficiency promotes the transport of amino acids, thus enhancing rapeseed adaptation to low phosphorus stress. Under the condition of potassium deficiency, we found that the expression of most *BnaAAT* DEGs was up-regulated in the shoots and most *BnaAAT* DEGs was down-regulated in the roots (Fig. 8). We speculated that increased amino acid content might help rapeseed respond to low phosphorus stress. In this study, we found that most *BnaAATs* were responded to B-deficiency and B-toxic. Therefore, we speculated that increased amino acid levels may help plants cope with boron defects and respond to boron toxicity. Under cadmium stress, it's worth noting that more *BnaAATs* were induced in the roots (Fig. 13), we speculated that the enhanced expression of *BnaAATs* might contribute to efficient AA transport and it further facilitated the biosynthesis of cadmium-chelators [43]. Consequently, it enhances the resistance of plants to cadmium toxicity. Soil salt stress is an extreme environmental abiotic stress with an adverse impact on plant growth and crop production worldwide [44]. It has been reported that proline transporters (ProTs) were induced under salt stress [45]. In *B. napus*, *BnaA4.ProT2* and *BnaC4.ProT1b* were strongly induced by salt stress in roots, while *BnaC3.ProT1* and *BnaA3.ProT1* were down-regulated in the shoots under the condition of salt stress (Fig. 12). *BnaC4.AAP1*, *BnaCn.AAP1*, *BnaA9.AAP1*, *BnaA4.CAT3*, *BnaA2.ATLb2*, *BnaA5.ATLb3*, *BnaA5.CAT4*, *BnaAn.CAT4*, *BnaC1.CAT4*, *BnaC2.ATLa3*, *BnaAn.ATLa3*, *BnaA5.ANT1*, *BnaA2.BAT1* and *BnaC2.BAT1* were significantly up-regulated in shoots by salt stress (Fig. 12). On the contrary, *BnaC3.AAP4*, *BnaA10.AAP5*, *BnaC6.AAP5*, *BnaA4.ATLa4*, *BnaCn.ATLa4*, *BnaA6.ANT3*, *BnaCn.ANT3*, *BnaC7.BAT1* and *BnaA6.BAT1a* were down-regulated in the roots by salt stress (Fig. 12). These results indicated that these *AATs* play important roles in response to the salt stress by adjusting the transport of amino acids.

Methods

Identification of members of the AAT gene family

Firstly, we used the AA sequences of AATs from *A. thaliana* as source sequences and conducted a BLASTp search for the AAP homologs in *B. napus*. Secondly, the protein sequences were submitted to InterProScan (<http://www.ebi.ac.uk/Tools/InterProScan/>) to confirm the existence of AAT domain (PF01490 and PF00324). Then, we removed protein sequences without AAT domain. Finally, all members of the *AAT* gene family were screened. The *AAT* gene sequences of other species were obtained in the same way. In this work, we get the *AAT* gene sequences using the following databases: The Arabidopsis Information Resource (TAIR10, <https://www.arabidopsis.org/>) for *A. thaliana*, Brassica Database (BRAD) v. 4.1 (<http://brassicadb.org/brad/>) for *B. napus*, *B. oleracea* and *B. rapa*, the MSU-RGAP (MSURice Genome Annotation Project) database (http://rice.plantbiology.msu.edu/analyses_search_domain.shtml) for rice.

Gene nomenclature of BnaAATs

In this work, according to the nomenclature previously reported [46], we renamed *AAT* genes in *Brassica* species based on the following criterion: genus (one capital letter) + plant species (two lowercase letters) + chromosome (followed by a period) + name of the *AAT* homologs in *A. thaliana*. For example, *BnaA8.CAT1* represents an *Arabidopsis CAT1* homolog on the chromosome A8 of *B. napus*.

Multiple sequence alignment and Phylogeny Analysis of BnaAATs

To analyze the evolutionary relationship, 203 *BnaAATs* sequences were aligned by ClustalW program in MEGA 10.2.2 with default settings. 12 neighbor-joining tree was then constructed based on the alignment result. 22 *BnaCATs* 9 *AtCATs*, 11 *OsCATs* and 31 *TaCATs* amino acid sequences were aligned by ClustalW program in MEGA 10.2.2 with default settings, and the Interactive Tree Of Life (iTOLv5) online tool (<https://itol.embl.de/>) was finally used to polish the NJ-tree [31].

Chromosome location and synteny analysis of BnaAATs

With chromosome length and gene position files, *BnaAATs* genes were mapped onto chromosomes using "Gene Location Visualize (Advanced)" of TBtools [47]. We used "One Step MCScanX" of TBtools to analyze *AAT* duplication events with genome sequences and gff3 files. The syntenic analysis maps of orthologous *AAT* genes were constructed using the Dual System Plotter software (<https://github.com/CJ-Chen/TBtools>) [47].

Analysis of evolutionary selection pressure and functional differentiation of BnaAATs

To verify positive or negative (purifying) selection pressure on *BnaAATs*, we calculated the values of K_a , K_s , and K_a/K_s . Firstly, we did pairwise alignment of the *BnaAAT-AtAAT* coding sequences (CDSs) in the Excel spreadsheet. Subsequently, we submitted the paired coding sequences (CDSs) sequences to the TBtools for the calculation of the K_a , K_s , and K_a/K_s with the yn00 method [48]. It is presented that $K_a/K_s > 1.0$ means positive selection, while $K_a/K_s < 1.0$

indicates purifying selection, and $K_a/K_s = 1.0$ denotes neutral selection, with reference to Darwin's evolution theory. According to the following formula: $T = K_s/2\lambda$; $\lambda = 1.5 \times 10^{-8}$, we calculated the divergence time of *BnaAATs* from their progenitors for *Brassicaceae* species [13].

Molecular characterization of BnaAATs

The molecular weight (MW, kD), isoelectric point (pI), grand average of hydropathy (GRAVY), and instability index (II) of BnaAATs were determined by ProtParam tool in ExPASy Server (<https://web.expasy.org/protparam/>) [49]. To investigate the characteristics of transmembrane helices of AtAATs and BnaAATs, we submitted the AA sequences of them to the TMHMMv.2.0 (<http://www.cbs.dtu.dk/services/TMHMM/>) program. We utilized STRING (Search Tool for Recurring Instances of Neighboring Genes) v 11.0 (<https://string-db.org>) web-server to retrieve and display recurring association networks, involving direct (physical) and indirect (function) association, of the AAT proteins in *A. thaliana* and *B. napus*. The online SignalP v. 4.1 (<http://www.cbs.dtu.dk/services/SignalP/>) [50] was used to predict the subcellular localization of BnaAATs.

Identification, conserved domain, gene structure and cis-acting regulatory elements (CREs) of AAT genes.

The conserved motifs of the *BnaAAT* genes were identified by the MEME Suite web server (<http://meme-suite.org/>). The number of motifs was set to 15, and all other parameters were the default ones. The gene structure and conserved domain were visualized via TBtools [47]. The 2000 bp upstream DNA sequence of the 5-UTR of the *BnaAAT* genes was selected as the promoter sequence. The promoter sequences were uploaded to the PlantCare database (<http://bioinformatics.psb.ugent.be/webtools/plantcare/html/>) to scan for cis-acting regulatory elements (CREs). The cis-acting regulatory elements (CREs) from the PlantCare database were subsequently screened manually and visualized via TBtools [47].

Transcriptional analysis of BnaAATs under diverse nutrient stresses.

To further identify the transcriptional responses of *BnaAATs* under multiple nutrient stresses, the uniform *B. napus* seedlings (Zhongshuang 11) after seed germination were transplanted into black plastic containers holding 10 L Hoagland nutrient solution, which contained 1.0 mM KH_2PO_4 , 5.0 mM KNO_3 , 5.0 mM $\text{Ca}(\text{NO}_3)_2 \cdot 4\text{H}_2\text{O}$, 2.0 mM $\text{MgSO}_4 \cdot 7\text{H}_2\text{O}$, 0.050 mM EDTA-Fe, 9.0 μM $\text{MnCl}_2 \cdot 4\text{H}_2\text{O}$, 0.80 μM $\text{ZnSO}_4 \cdot 7\text{H}_2\text{O}$, 0.30 μM $\text{CuSO}_4 \cdot 5\text{H}_2\text{O}$, 0.10 μM $\text{Na}_2\text{MoO}_4 \cdot 2\text{H}_2\text{O}$, and 46 μM H_3BO_3 . The rapeseed seedlings were cultivated for 10 days (d) in a chamber under the following conditions: light intensity of $300\text{--}320 \mu\text{mol m}^{-2} \text{s}^{-1}$, temperature of 25°C daytime/22°C night, light period of 16h photoperiod/ 8 h dark, and relative humidity of 70%. For the low nitrate treatment, the 7-d-old uniform *B. napus* seedlings after germination were hydroponically cultivated under high (6.0 mM) nitrate for 10 d, and then were transferred into low (0.30 mM) nitrate solution for 3 d. For the inorganic phosphate (Pi) starvation treatment, the 7-d-old uniform *B. napus* seedlings after seed germination were first hydroponically grown under 250 μM phosphate (KH_2PO_4) for 10 d, and then were transferred to 5 μM phosphate for 3 d. For the potassium deficiency treatment, the 7-d-old uniform rapeseed seedlings after seed germination were hydroponically cultivated under high (6.0 mM) potassium for 10 d and then were transferred to low (0.05 mM) potassium for 3 d. For the low born (B) treatment, *B. napus* seedlings after seed germination were first hydroponically grown under 10 μM H_3BO_3 for 10 d, and then were transferred to 0.25 μM H_3BO_3 for 3 d until sampling. For the born (B) toxicity treatment, *B. napus* seedlings after seed germination were first hydroponically grown under 10 μM H_3BO_3 for 10 d, and then were transferred to 25 μM H_3BO_3 for 3 d until sampling. For the ammonium (NH_4^+) toxicity treatment, the 7-d-old uniform *B. napus* seedlings after seed germination were hydroponically cultivated under high nitrate (6.0 mM) for 10 d, and then were transferred to N-free condition for 3 d. Finally, the above seedlings were sampled after exposure to 9.0 mM ammonium for 3 d. For the salt stress treatment, the 7-d-old uniform *B. napus* seedlings after seed germination were hydroponically cultivated in a NaCl-free solution for 10 d, subsequently were transferred to 200 mM NaCl for 1 d. For the cadmium (Cd) toxicity treatment, the 7-d-old uniform *B. napus* seedlings after seed germination were hydroponically cultivated in a Cd-free solution for 10 d, and then were grown under 10 μM CdCl_2 for 1 d.

Abbreviations

AA: amino acid;

AAP: amino acid permease;

AAT: amino acid transporter;

CAT: cationic amino acid transporter;

ACT: amino acid/choline transporter;

PHS: polyamine H+-symporter;

GAT: comprises caminobutyric acid transporter;

ProT: proline transporter;

LHT: lysine and histidine transporter;

AUX: auxin transporters;

ANT: aromatic and neutral amino acid transporter;

ATL: amino acid transporter-like;

TTP: tyrosine-specific transporter;

At: Arabidopsis thaliana;

Athaliana: Arabidopsis thaliana;

B: boron;

Bna: Brassica napus;

Bol: Brassica oleracea;

Bra: Brassica rapa;

BRAD: Brassica Database;

Cd: cadmium;

CRE: cis-acting regulatory element;

DEGs: differentially expressed genes;

N: nitrogen;

NH₄⁺: ammonium;

NO₃⁻: nitrate;

NUE: nitrogen use efficiency;

Pi: phosphate;

K: potassium;

B: boron;

TAIR; The Arabidopsis Information Resource.

Declarations

Ethics approval and consent to participate

Not applicable.

Consent for publication

Not applicable.

Availability of data and materials

All the data and materials that are required to reproduce these findings can be shared by contacting the corresponding author, Dr Ying-peng Hua (yingpenghua@zzu.edu.cn). The transcriptome sequencing data were deposited with the Bioproject of PRJNA340053 under the SRA database

Competing interests

The authors declare that they have no competing interests.

Funding

This study was financially supported by the National Natural Science Foundation of China (Grant NO. 31801923). The funder was not involved in the experimental design of the study, data collection, analysis and interpretation, and in writing the manuscript.

Authors' contributions

HYP, ZT and HJY was involved in data interpretation. KXC and ZTY cultivated the rapeseed plants, and made the experiments. HJY and HYP designed the study, and KXC and YCP wrote the manuscript. All the authors read and approved the final version of the manuscript.

Acknowledgements

Not applicable.

References

1. O'Brien JA, Vega A, Bouguyon E, Krouk G, Gojon A, Coruzzi G, Gutiérrez RA. Nitrate transport, sensing, and responses in plants. *Mol Plant*. 2016; 9: 837–856.
2. Yang GZ, Wei QX, Huang H, Xia JX. Amino acid transporters in plant cells: A Brief Review. *Plants*. 2020; 9: 967.
3. Wipf D, Ludewig U, Tegeder M, Rentsch D, Koch W, Frommer WB. Conservation of amino acid transporters in fungi, plants and animals. *Trends Biochem Sci*. 2002; 27: 139–147.
4. Sheng L, Deng L, Yan HW, Zhao Y, Dong Q, Jiang HY, et al. A genome-wide analysis of the AAP gene family in maize. *J Proteomics & Bioinformatics*. 2014; 7:1.
5. Lee YH, Foster J, Chen J, Voll LM, Weber APM, Tegeder M. AAP1 transports uncharged amino acids into roots of Arabidopsis. *Plant J*. 2007; 50: 305–319.
6. Zheng LW, Ma SJ, Zhou T, Yue CP, Hua YP, Huang JY. Genome-wide identification of Brassicaceae B-BOX genes and molecular characterization of their transcriptional responses to various nutrient stresses in allotetraploid rapeseed. *BMC Plant Biol*. 2021; 21: 288.
7. Wang X, Han YP, You CX, Wang XF, Hao YJ. Identification, comparison and expression analysis of cationic amino acid transporter (CAT) in apple. *Plant Physiol J*. 2020; 56: 2631–2646.
8. Yang HY, Krebs M, Stierhof Y, Ludewig U: Characterization of the putative amino acid transporter genes AtCAT2, 3 & 4: The tonoplast localized AtCAT2 regulates soluble leaf amino acids. *J Plant Physiol*. 2014; 171: 594–601.
9. Yang YW, Yang LT, Li ZG. Molecular cloning and identification of a putative tomato cationic amino acid transporter-2 gene that is highly expressed in stamens. *Plant Cell, Tissue and Organ Culture (PCTOC)*. 2013; 112(1): 55–63.
10. Chalhou B, Denoed F, Liu S, Parkin IA, Tang H, Wang X, Chiquet J, Belcram H, Tong C, Samans B et al. Plant genetics. Early allopolyploid evolution in the post-Neolithic *Brassica napus* oilseed genome. *Science*. 2014; 345(6199): 950–953.
11. Avice JC, Etienne P. Leaf senescence and nitrogen remobilization efficiency in oilseed rape (*Brassica napus* L.). *J Exp Bot*. 2014; 65(14): 3813–3824.
12. Xu GX, Guo C, Shan HY, Kong HZ. Divergence of duplicate genes in exon-intron structure. *P Proc Natl Acad Sci U S A*. 2012; 109(4): 1187–1192.
13. Blanc G, Wolfe KH. Widespread paleopolyploidy in model plant species inferred from age distributions of duplicate genes. *Plant Cell*. 2004; 16(7):1667–1678.
14. Duan Y, Zhu XJ, Shen JZ, Xing HQ, Zhou ZW, Ma YC. Genome-wide identification, characterization and expression analysis of the amino acid permease gene family in tea plants (*Camellia sinensis*). *Genomics*. 2020; 112: 2866–2874.
15. Perchlik M, Tegeder M. Improving plant nitrogen use efficiency through alteration of amino acid transport processes. *Plant Physiol*. 2017; 175(1): 235–247.
16. Borsani G, Bassi MT, Sperandeo MP, Grandi AD, Buoninconti A, Riboni M, Manzoni M, Incerti B, Pepe A, Andria G et al. *SLC7A7*, encoding a putative permease-related protein, is mutated in patients with lysinuric protein intolerance. *Nat Genet*. 1999; 21(3): 297–301.
17. Zhang ZH, Zhou T, Liao Q, Yao JY, Liang GH, Song HX, Guan CY, Hua YP. Integrated physiologic, genomic and transcriptomic strategies involving the adaptation of allotetraploid rapeseed to nitrogen limitation. *BMC Plant Biol*. 2018; 18: 322.
18. DING L, WANG KJ, JIANG GM, BISWAS DK, XU H, LI LF, LI YH. Effects of nitrogen deficiency on photosynthetic traits of maize hybrids released in different years. *Ann Bot*. 2005; 96(5): 925–930.
19. Gan HH, Jiao Y, Jia J, Wang XL, Li H, Shi WG, Peng CH, Polle A, Luo ZB. Phosphorus and nitrogen physiology of two contrasting poplar genotypes when exposed to phosphorus and/or nitrogen starvation. *Tree Physiol*. 2016; 36(1): 22–38.
20. Musavizadeh Z, Najafi-Zarrini H, Kazemitabar SK, Hashemi SH, Faraji S, Barcaccia G, Heidari P. Genome-wide analysis of potassium channel genes in rice: expression of the *OsAKT* and *OsKAT* genes under salt stress. *Genes-Basel* 2021; 12(5): 784.
21. Amrutha RN, Sekhar PN, Varshney RK, Kishor PBK. Genome-wide analysis and identification of genes related to potassium transporter families in rice (*Oryza sativa* L.). *Plant Sci*. 2007; 172(4): 708–721.
22. Ashley MK, Grant M, Grabov A. Plant responses to potassium deficiencies: a role for potassium transport proteins. *J Exp Bot*. 2006; 57(2): 425–436.
23. Wei W, Hu Y, Han YT, Zhang K, Zhao FL, Feng JY. The WRKY transcription factors in the diploid woodland strawberry *Fragaria vesca*: Identification and expression analysis under biotic and abiotic stresses. *Plant Physiol Biochem*. 2016; 105:129–44.
24. Liu Y, von Wirén N. Ammonium as a signal for physiological and morphological responses in plants. *J Exp Bot*. 2017; 68(10): 2581–2592.
25. He JX, Zhuang YF, Li C, Sun X, Zhou HP, et al. SIMP1 modulates salt tolerance by elevating ERAD efficiency through UMP1A-mediated proteasome maturation in plants. *New Phytol*. 2021; 232(2): 625–641.
26. Zhang Y, Chao JT, Li XC, Zhang C, Khan R, Shi Y, et al. Comparative transcriptome combined with biochemical and physiological analyses provide new insights toward cadmium accumulation with two contrasting *Nicotiana* species. *Physiol Plant*. 2021; 173(1): 369–383.
27. Zhao HM, Ma HL, Yu L, Wang X, Zhao J. Genome-wide survey and expression analysis of amino acid transporter gene family in rice (*Oryza sativa* L.). *PloS One*. 2012; 7(11): e49210.
28. Wan YF, King R, Mitchell RAC, Hassani-Pak K, Hawkesford MJ. Spatiotemporal expression patterns of wheat amino acid transporters reveal their putative roles in nitrogen transport and responses to abiotic stress. *Sci Rep*. 2017; 7(1): 5461.
29. Ma HL, Cao XL, Shi SD, Li SL, Gao JP, Ma YL, Zhao Q, Chen Q. Genome-wide survey and expression analysis of the amino acid transporter superfamily in potato (*Solanum tuberosum* L.). *Plant Physiol Biochem*. 2016; 107: 164–177.

30. Cui JQ, Hua YP, Zhou T, Liu Y, Huang JY, Yue CP. Global landscapes of the *Na⁺/H⁺ antiporter (NHX)* family members uncover their potential roles in regulating the rapeseed Resistance to salt stress. *Int J Mol Sci.* 2020; 21(10): 3429.
31. Su DD, Xiang W, Wen L, Lu W, Shi Y, Liu YD, Li ZG. Genome-wide identification, characterization and expression analysis of BES1 gene family in tomato. *BMC Plant Biol.* 2021; 21(1): 161.
32. Cheng L, Yuan HY, Ren R, Zhao SQ, Han YP, Zhou QY, Ke DX, Wang YX, Wang L. Genome-wide identification, classification, and expression analysis of amino acid transporter gene family in *Glycine max*. *Front Plant Sci.* 2016; 7: 515.
33. Wu XM, Kou SJ, Liu YL, Fang YN, Xu Q, Guo WW. Genomewide analysis of small RNAs in nonembryogenic and embryogenic tissues of citrus: microRNA- and siRNA-mediated transcript cleavage involved in somatic embryogenesis. *Plant Biotechnol J.* 2015; 13(3): 383–394.
34. Aan Den Toorn M, Albrecht C, de Vries S. On the Origin of SERKs: Bioinformatics Analysis of the Somatic Embryogenesis Receptor Kinases. *Mol Plant.* 2015; 8(5):762–782.
35. Zhou T, Yue CP, Huang JY, Cui JQ, Liu Y, Wang WM, Tian C, Hua YP. Genome-wide identification of the amino acid permease genes and molecular characterization of their transcriptional responses to various nutrient stresses in allotetraploid rapeseed. *BMC Plant Biol.* 2020; 20: 151.
36. Lynch M, Conery JS. The evolutionary fate and consequences of duplicate genes. *Science.* 2000; 290(5494): 1151–1155.
37. Chalhoub B, Denoeud F, Liu SY, Parkin IA, Tang HB, Wang XY, Chiquet J, Belcram H, Tong C, Samans B et al. Plant genetics. Early allopolyploid evolution in the post-Neolithic *Brassica napus* oilseed genome. *Science.* 2014; 345(6199): 950–953.
38. Santiago JP, Tegeder M. Connecting source with sink: the role of Arabidopsis AAP8 in phloem loading of amino acids. *Plant Physiol.* 2016; 171(1): 508–521.
39. Couturier J, Doidy J, Guinet F, Wipf D, Blaudez D, Chalot M. Glutamine, arginine and the amino acid transporter Pt-CAT11 play important roles during senescence in poplar. *Ann Bot.* 2010; 105(7): 1159–1169.
40. Svennerstam H, Jamtgard S, Ahmad I, Huss-Danell K, Nasholm T, Ganeteg U. Transporters in Arabidopsis roots mediating uptake of amino acids at naturally occurring concentrations. *New Phytol.* 2011; 191(2): 459–467.
41. Gerendás J, Ratcliffe RG. Intracellular pH regulation in maize root tips exposed to ammonium at high external pH. *J Exp Bot* 2000, 51(343):207–219.
42. Cruz C, Bio AFM, Domínguez-Valdivia MD, Aparicio-Tejo PM, Lamsfus C, Martins-Loução MA. How does glutamine synthetase activity determine plant tolerance to ammonium? *Planta.* 2006; 223(5): 1068–1080.
43. Sun SK, Xu XJ, Tang Z, Tang Z, Huang XY, Wirtz M, Hell R, Zhao FJ. A molecular switch in sulfur metabolism to reduce arsenic and enrich selenium in rice grain. *Nat Commun.* 2021; 12(1): 1392.
44. Zhu JK. Abiotic stress signaling and responses in plants. *Cell.* 2016; 167(2): 313–324.
45. Rentsch D, Hirner B, Schmelzer E, Frommer, WB. Salt stress-induced proline transporters and salt stress-repressed broad specificity amino acid permeases identified by suppression of a yeast amino acid permease-targeting mutant. *Plant Cell.* 1996; 8(8): 1437–1446.
46. Ostergaard L, King GJ. Standardized gene nomenclature for the Brassica genus. *Plant Methods.* 2008; 4(1): 10.
47. Chen CJ, Chen H, Zhang Yi, Thomas HR, Frank MH, He YH, Xia R. TBtools: an integrative toolkit developed for interactive analyses of big biological data. *Mol Plant.* 2020; 13(8): 1194–1202.
48. Yang Z, Nielsen R. Estimating synonymous and nonsynonymous substitution rates under realistic evolutionary models. *Mol Biol Evol.* 2000; 17(1): 32–43.
49. Wilkins MR, Gasteiger E, Bairoch A, Sanchez JC, Williams KL, Appel RD, Hochstrasser DF. Protein identification and analysis tools in the ExpASY server. *Methods Mol Biol.* 1999; 112:531–552.
50. Horton P, Park KJ, Obayashi T, Fujita N, Harada H, Adams-Collier CJ, Nakai K. WoLF PSORT: protein localization predictor. *Nucleic Acids Res.* 2007; 35(Web Server): W585-W587.

Tables

Table 1 Identification of the *amino acid transporters (AATs)* genes in *Arabidopsis* and three *Brassica* species

Group	<i>Arabidopsis thaliana</i> (125 Mb)	<i>Brassica rapa</i> (465 Mb)	<i>Brassica oleracea</i> (485 Mb)	<i>Brassica napus</i> (1130 Mb)
AAP	8	19	17	34
LHT	10	14	14	28
GAT	2	3	3	6
ProT	3	6	5	12
AUX	4	10	9	18
ANT	4	5	6	10
ATLa	5	11	12	24
ATLb	10	12	16	27
CAT	9	13	13	22
ACT	1	3	2	5
PHS	5	7	7	13
TTP	2	2	3	4
Total	63	105	107	203

Figures

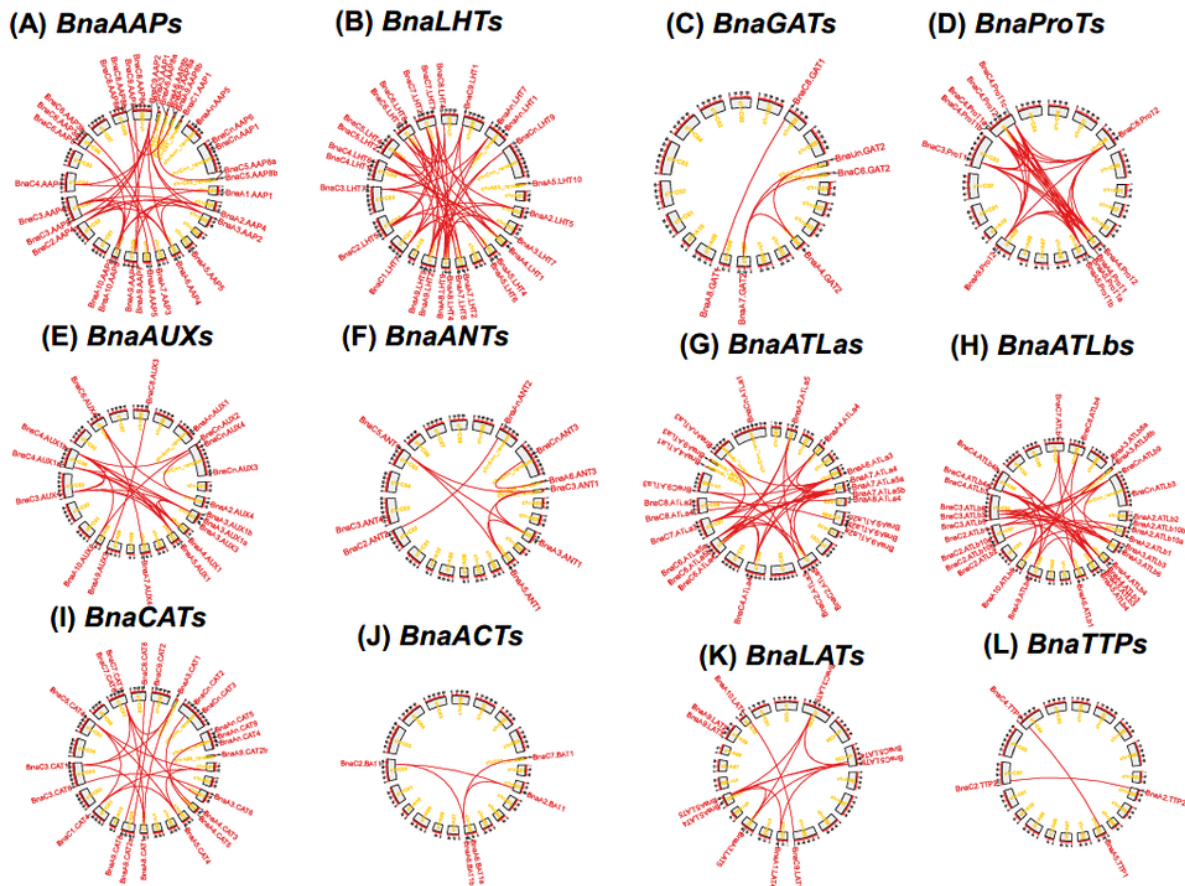


Figure 1
 Physical mapping and syntentic analysis of the *amino acid transporter* (AAT) family genes in *Brassica napus*. The different subfamilies AAPs (A), LHTs (B), GATs (C), ProTs (D), AUXs (E), ANTs (F), ATLAs (G), ATLbs (H), CATs (I), ACTs (J) LATs (K) and TTPs (L) chromosomal distribution and interchromosomal relationship of *BnaAAT* genes. The red lines indicate the duplicated AAT gene pairs.

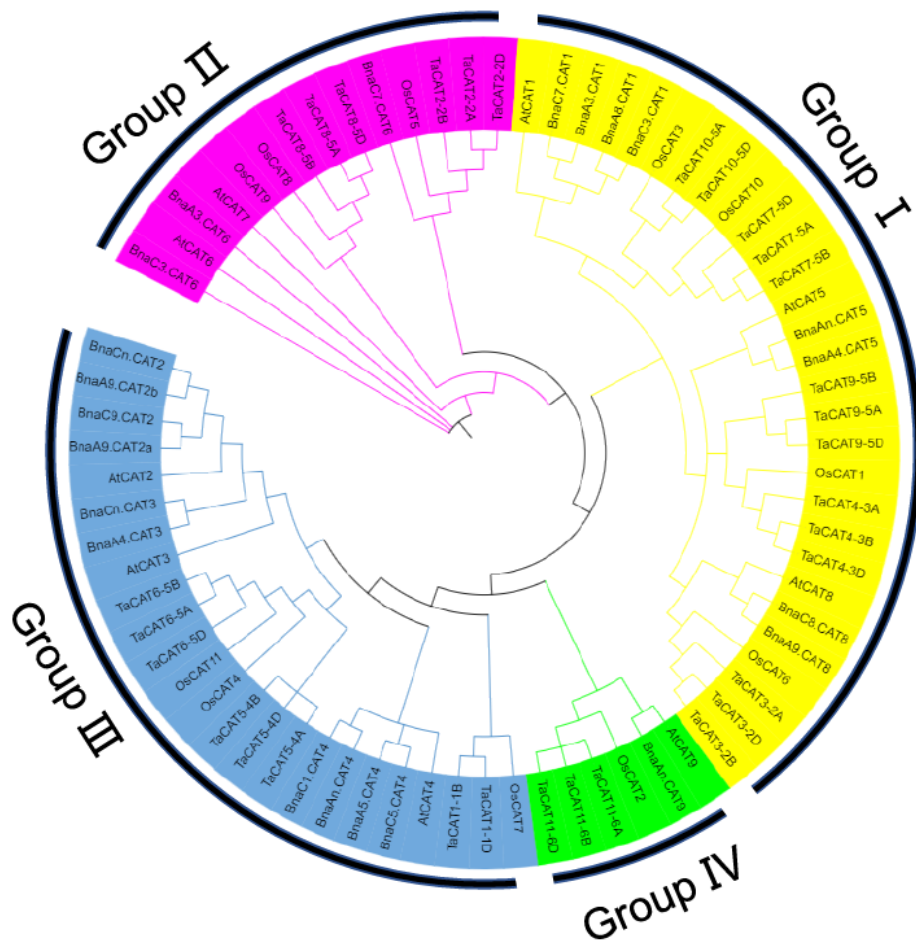


Figure 2

Phylogeny analysis of the cationic amino acid transporters (CATs) in *Arabidopsis thaliana*, *Brassica napus*, *Oryza sativa* and *wheat*. The CAT protein sequences were multi-aligned using the ClustalW program, and then an unrooted phylogenetic tree was constructed using MEGA 10.2.2 with the neighbor-joining method. Overall, 22 BnaCATs from *B. napus*, 9 AtCATs from *A. thaliana*, 31 TaeCATs from *wheat* and 11 OsaCATs from *Oryza sativa* were clustered into four groups (Group I-IV) based on high bootstrap values signified with different background colors.

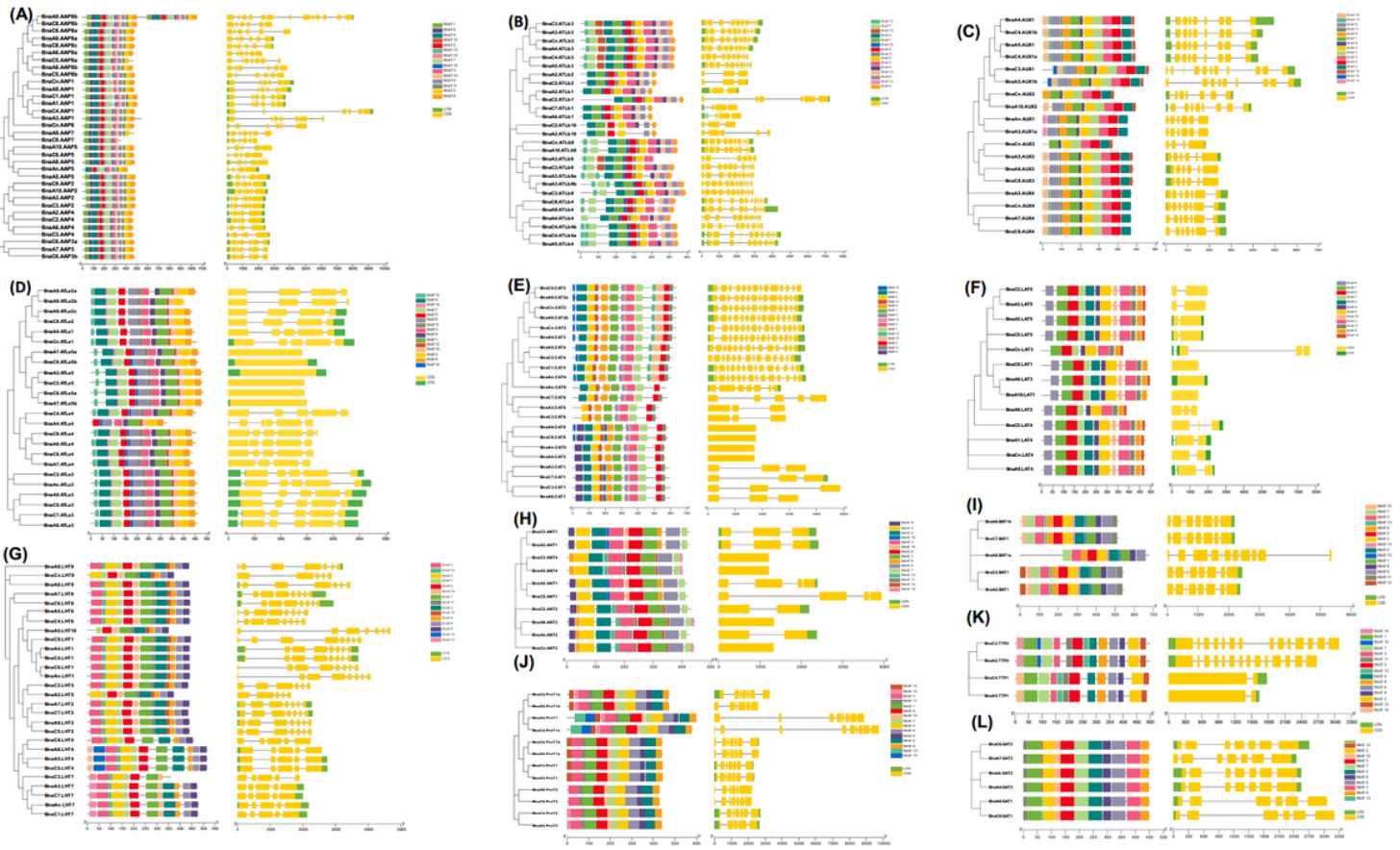


Figure 3

Phylogenetic relationships, architecture of conserved protein motifs, and gene structure of *BnaAAT* genes in each subfamily. Phylogenetic tree based on the *BnaAAT* sequences. Different colored boxes display different motifs. The exon-intron structure of *BnaAATs*. Green boxes indicate UTR regions, yellow boxes indicate exons, blackish-grey lines indicate introns. The bottom scale shows the protein length.

Figure 5

Specific expression patterns of (A), (B), (C), (D), (E), (F), (G), (H), (I), (J), (K), (L) *amino acid transporters* (AATs) in different *Brassica napus* organs scaled. Including bud, new pistil, blossomy pistil, wilting pistil, ovule, root, silique, stamen, leaf, sepal, pericarp, stem.

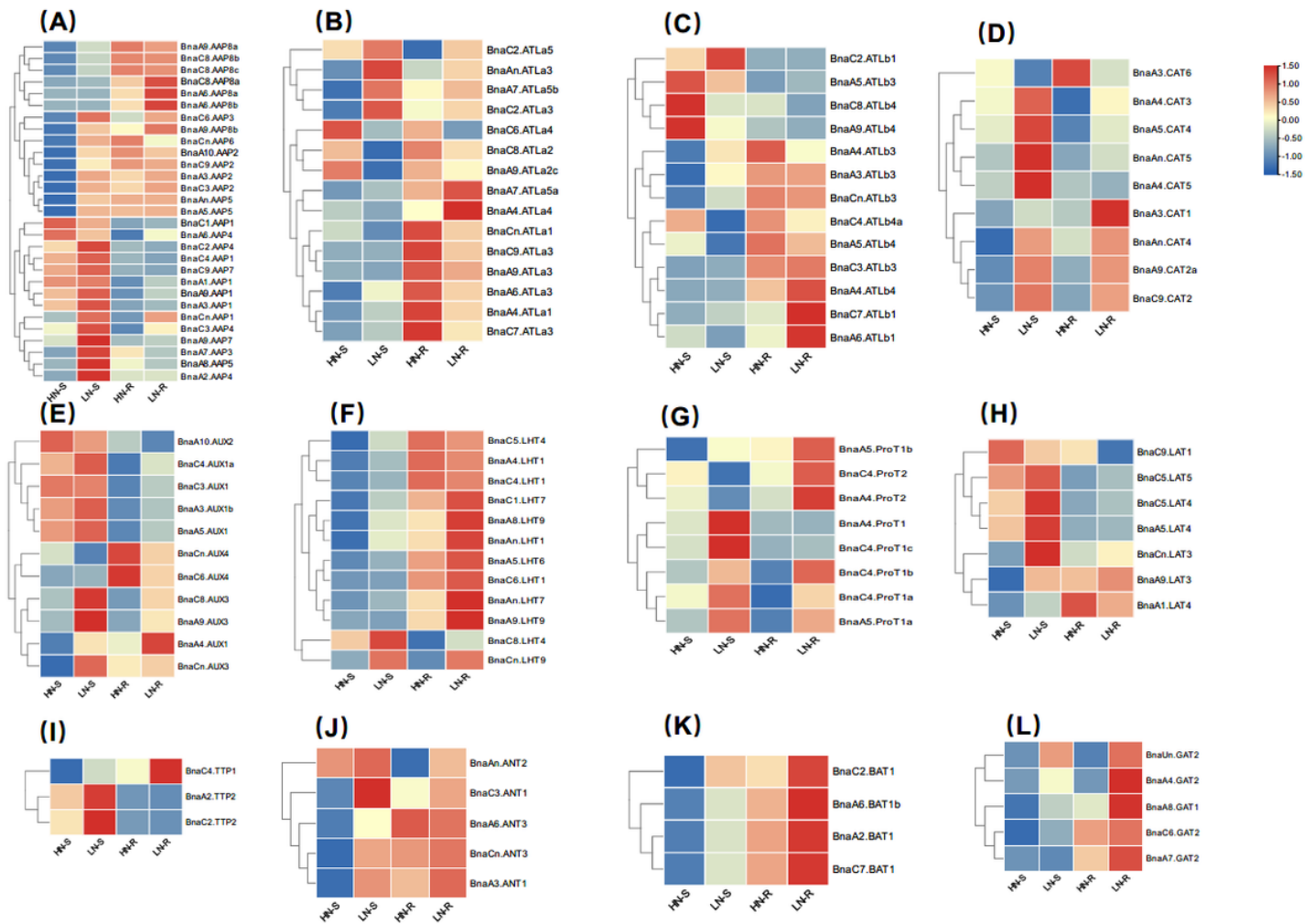


Figure 6

Transcriptional characterization of *amino acid transporters* (AATs) in rapeseed under the condition of HN and LN. Differential expression of AAPs (A), ATLas (B), ATLbs (C), CATs (D), AUXs (E), LHTs (F), ProTs (G), LATs (H), TTPs (I), ANTs (J), BATs (K) and GATs (L), under HN and LN conditions. For the low nitrate treatment, the 7 d-old uniform rapeseed seedlings were hydroponically cultivated under high (6.0 mM) nitrate for 10 d, and then were developed under low (0.30 mM) nitrate for 3 d until sampling. The shoots and roots were sampled, respectively. And each sample contains three independent biological replicates. The significance level of $p < 0.05$ is used as the threshold to identify AATs expression under the condition of high nitrate and low nitrate.

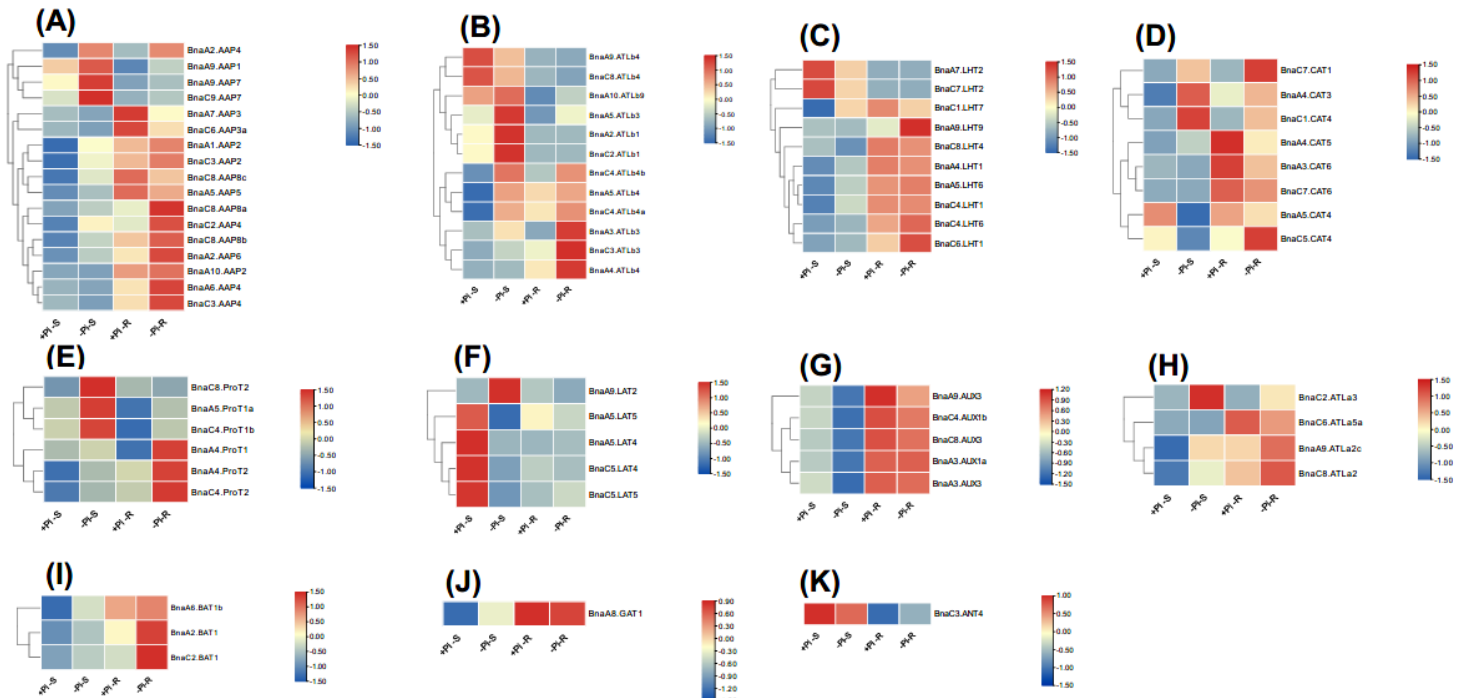


Figure 7

Transcriptional characterization of *amino acid transporters* (AATs) in rapeseed under the condition of HP and LP. Differential expression of the AATs (A), ATLBs (B), LHTs (C), CATs (D), ProTs (E), LATs (F), AUXs (G), ATLas (H), BATs (I), GATs (J) and ANTs (K) under the condition of high (+, 250 μM) phosphate and low (-, 5 μM) phosphate. For the transcriptional analysis, the 7-d-old uniform *B. napus* seedlings after germination were hydroponically cultivated under 250 μM phosphate (KH_2PO_4) for 10 d, and then were developed under 5 μM phosphate for 3 d until sampling. The shoots and roots were sampled, respectively. And each sample contains three independent biological replicates. The significance level of $P < 0.05$ is used as the threshold to identify the differential *BnaAATs* expression under the condition of high phosphate and low phosphate.

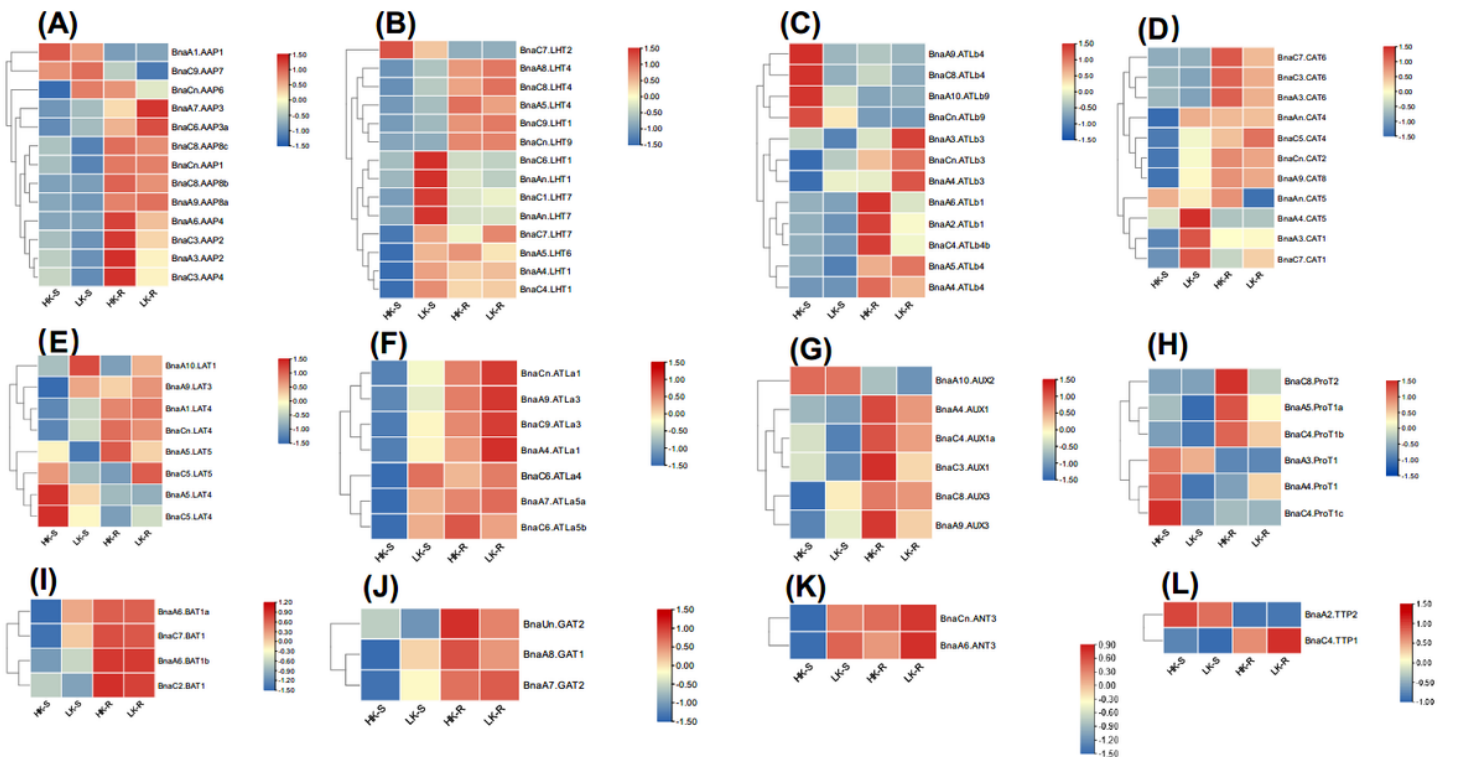


Figure 8

Transcriptional characterization of amino acid transporters (AATs) in rapeseed under the condition of HK and LK. Differential expression of *AAPs* (A), *LHTs* (B), *ATLbs* (C), *CATs* (D), *LATs* (E), *ATLas* (F), *AUXs* (G), *ProTs* (H), *BATs* (I), *GATs* (J), *ANTs* (K) and *TTPs* (L), under different potassium (K) levels. For the potassium deficiency treatment, the 7 d-old uniform rapeseed seedlings were hydroponically cultivated under high (6.0 mM) potassium for 10 d, and then were transferred to low (0.30 mM) potassium for 3 d until sampling. The shoots and roots were sampled, respectively. And each sample contains three independent biological replicates. The significance level of $p < 0.05$ is used as the threshold to identify *AATs* expression under different potassium (K) levels.

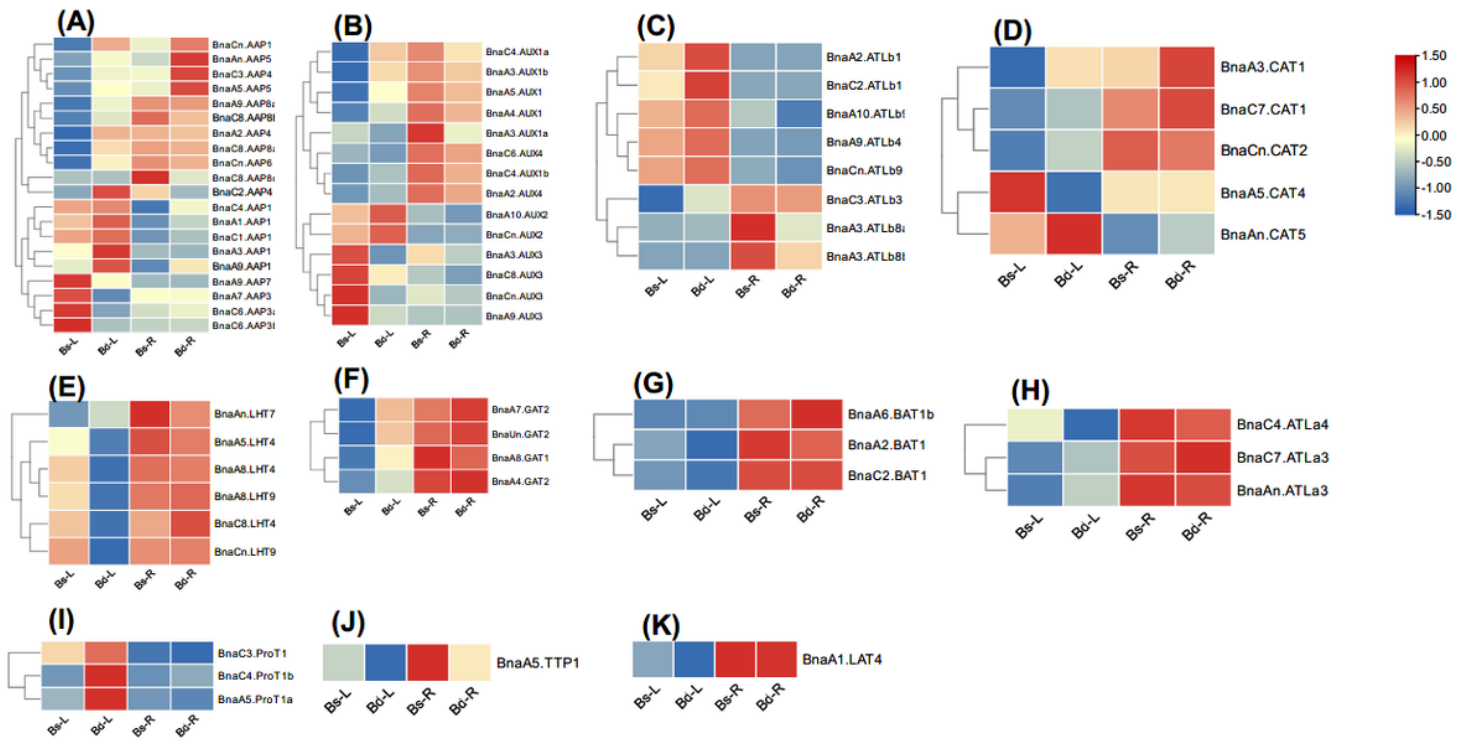


Figure 9

Transcriptional characterization of *amino acid transporters* (AATs) in rapeseed under the condition of low and normal boron. Differential expression of the *AAPs* (A), *AUXs* (B), *ATLbs* (C), *CATs* (D), *LHTs* (E), *GATs* (F), *BATs* (G), *ATLas* (H), *ProTs* (I), *TTPs* (J) and *LATs* (K) under normal (+, 10 μM) and low (-, 0.25 μM) boron supply levels. For the transcriptional analysis, the 7-d-old uniform *B. napus* seedlings were hydroponically grown under 10 μM H_3BO_3 for 10 d, and then were cultivated 0.25 μM H_3BO_3 for 3 d until sampling. The shoots and roots were sampled, respectively. And each sample contains three independent biological replicates. The significance level of $P < 0.05$ is used as the threshold to identify the differential *BnaAATs* expression under the condition of high boron and low boron.

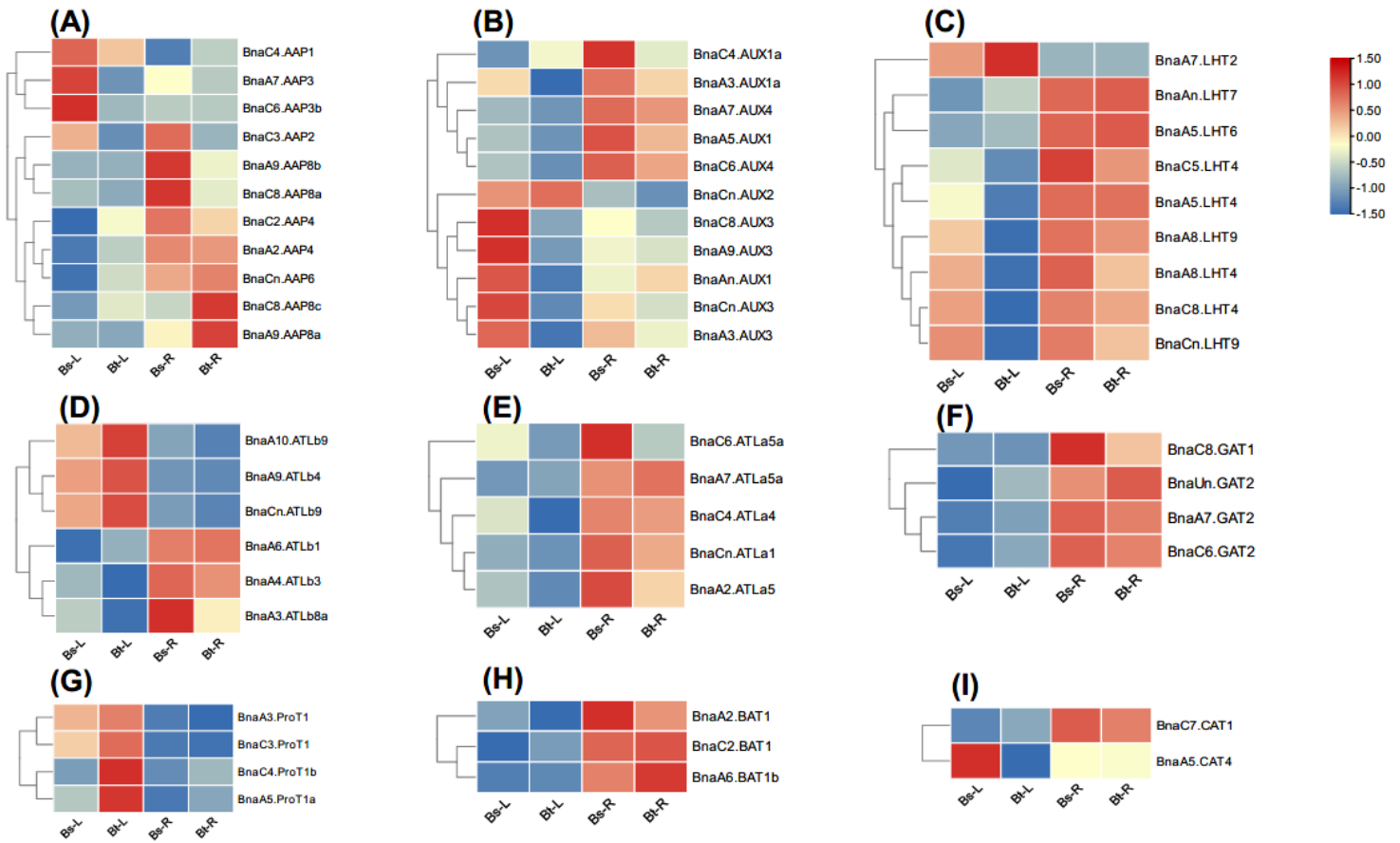


Figure 10

Transcriptional characterization of *amino acid transporters* (AATs) in rapeseed under the condition of high and normal boron. Differential expression of the AAPs (A), AUXs (B), LHTs (C), ATLBs (D), ATLas (E), GATs (F), ProTs (G), BATs (H), CATs (I) under normal (+, 10 μM) and high (+, 25 μM) boron supply levels. For the transcriptional analysis, the 7-d-old uniform *B. napus* seedlings were hydroponically grown under 10 μM H_3BO_3 for 10 d, and then were cultivated under 25 μM H_3BO_3 for 3 d until sampling. The shoots and roots were sampled, respectively. And each sample contains three independent biological replicates. The significance level of $P < 0.05$ is used as the threshold to identify the differential *BnaAATs* expression under the condition of high boron and low boron.

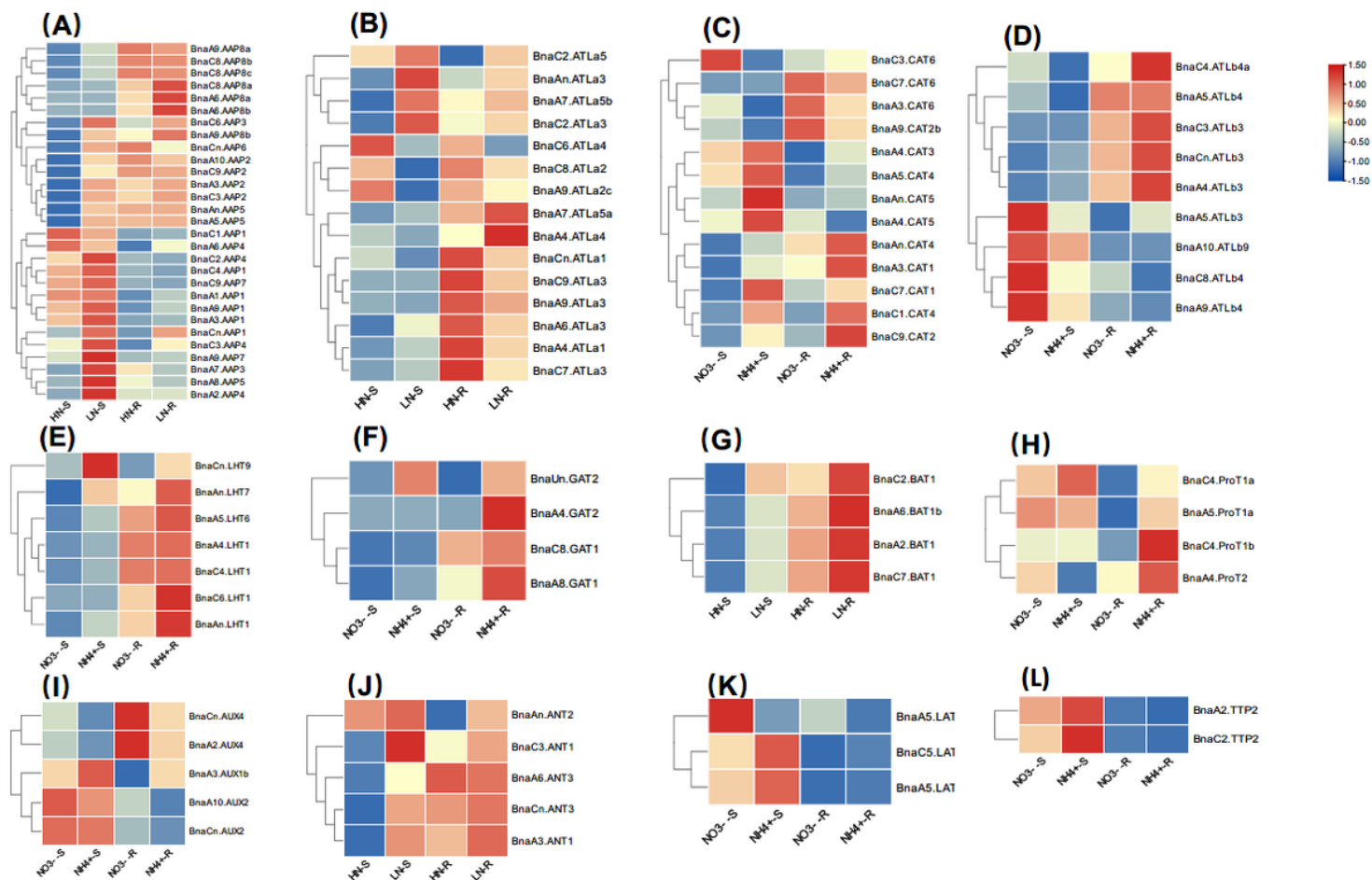


Figure 11

Transcriptional characterization of *amino acid transporters* (AATs) in rapeseed under different forms of N conditions. Differential expression of the AAPs (A), ATLAs (B), CATs (C), ATLbs (D), LHTs (E), GATs (F), BATs (G), ProTs (H), AUXs (I), ANTs (J), LATs (K) and TTPs (L) under nitrate (NO₃⁻) and ammonium (NH₄⁺) conditions. For the nitrate and ammonium treatment, the 7 d-old uniform rapeseed seedlings were hydroponically cultivated under 6.0 mM nitrate for 10 d, and subsequently were cultivated under N-free nutrient solution for 3 d. Then, 6.0 mM ammonium for 3 d until sampling. The shoots and roots were sampled, respectively. And each sample contains three independent biological replicates. The significance level of $p < 0.05$ is used as the threshold to identify the differential *BnaAATs* expression under nitrate (NO₃⁻) and ammonium (NH₄⁺) conditions.

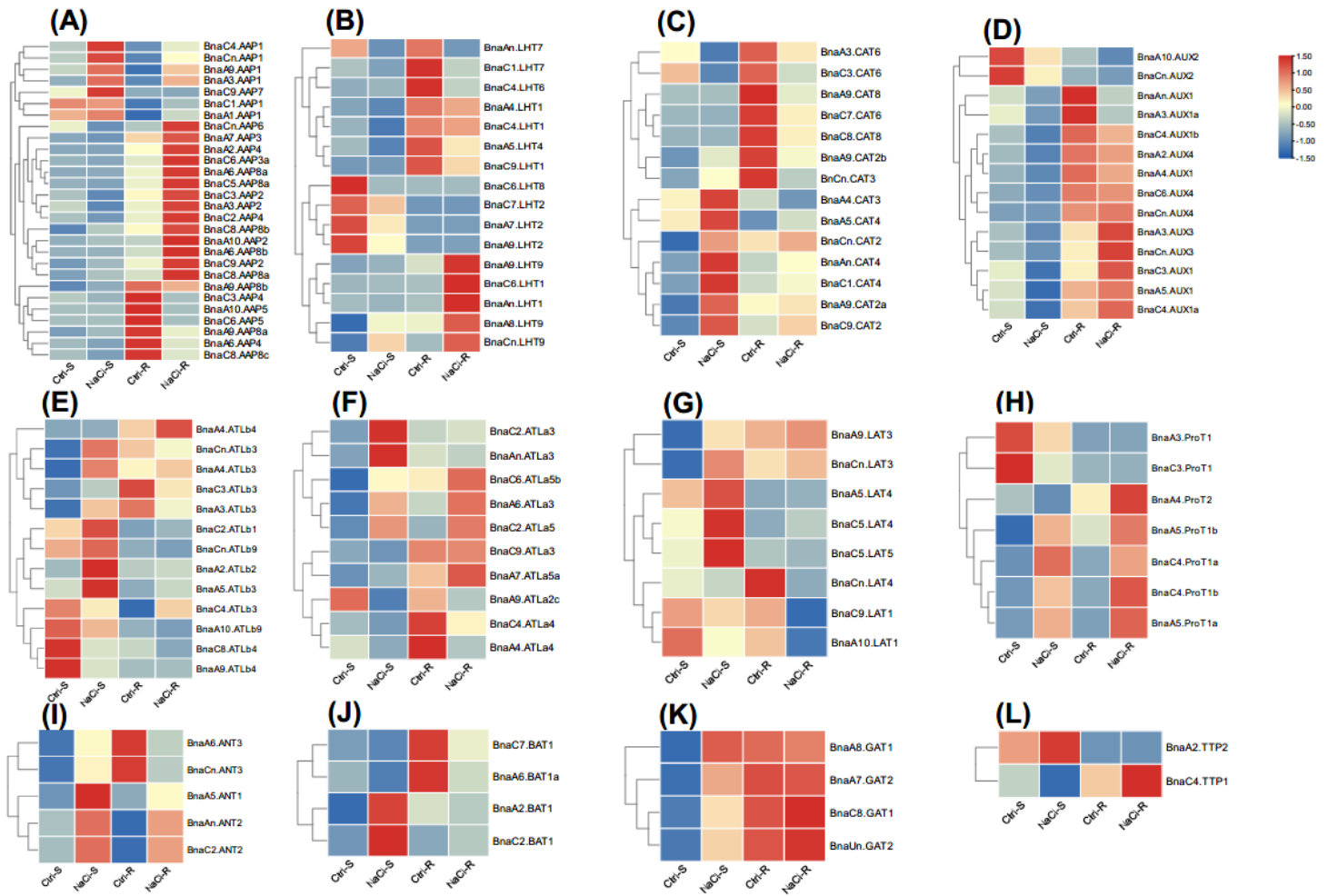


Figure 12

Transcriptional characterization of *amino acid transporters (AATs)* in rapeseed under salt stress. Differential expression of the *AAPs* (A), *LHTs* (B), *CATs* (C), *AUXs* (D), *ATLbs* (E), *ATLas* (F), *LATs* (G), *ProTs* (H), *ANTs* (I), *BATs* (J), *GATs* (K) and *TTPs* (L), under salt stress. For the salt stress treatment, the 7-d-old uniform rapeseed seedlings were hydroponically cultivated in a NaCl-free nutrient solution for 10 d, and then were transferred to 200 mM NaCl for 12h until sampling. The shoots and roots were sampled, respectively. And each sample contains three independent biological replicates. The significance level of $p < 0.05$ is used as the threshold to identify *AATs* expression under salt stress.

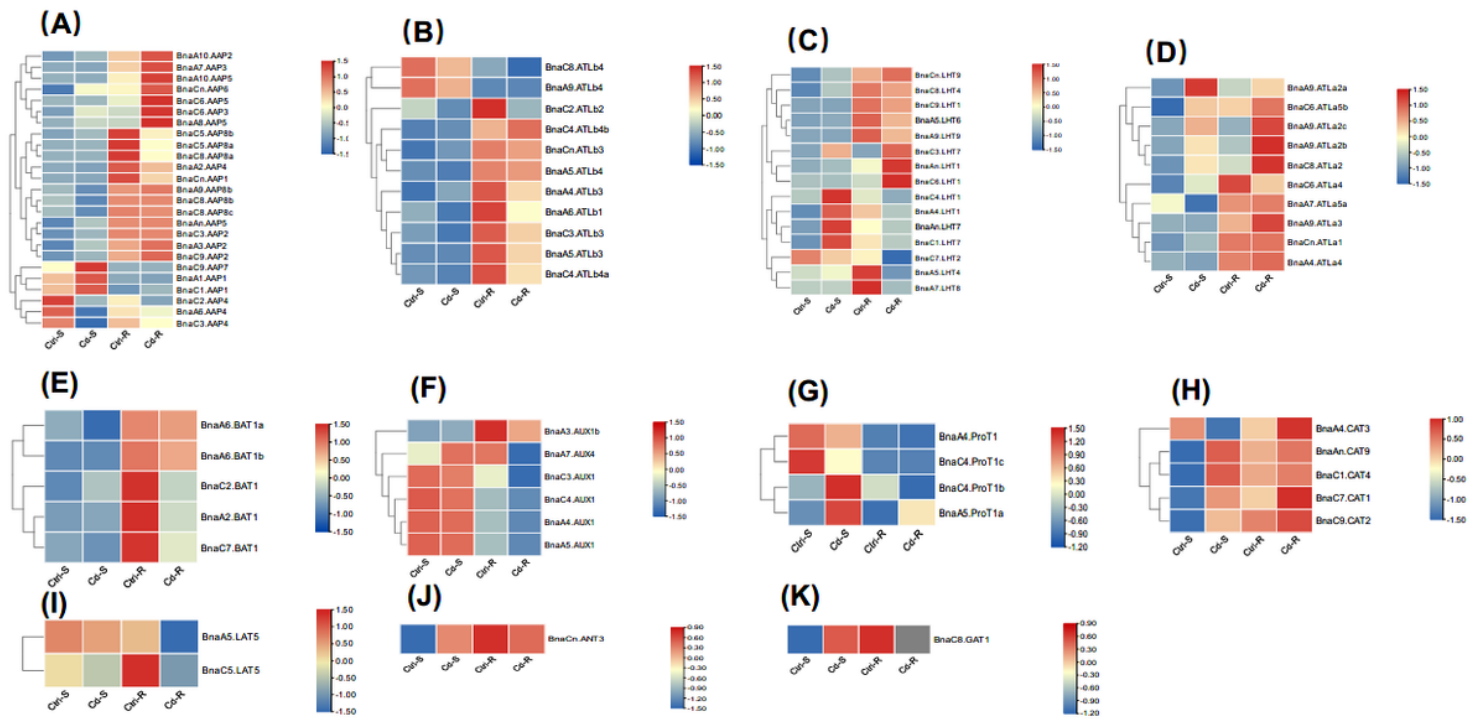


Figure 13

Transcriptional characterization of *amino acid transporters (AATs)* in *Brassica napus* under cadmium (Cd) toxicity. Differential expression of the *AAPs* (A), *ATLbs* (B), *LHTs* (C), *ATLas* (D), *BATs* (E), *AUXs* (F), *ProTs* (G), *CATs* (H), *LATs* (I), *ANTs* (J), and *GATs* (K) under Cd-free (-Cd) and Cd (10 μM CdCl₂) toxicity. For the transcriptional analysis, the 7-d-old uniform *B. napus* seedlings were hydroponically cultivated in a cadmium-free solution for 10 d, and then were grown under 10 μM CdCl₂ for 12 h. The shoots and roots were sampled, respectively. And each sample includes three independent biological replicates. The significance level of $P < 0.05$ is used as the threshold to identify the differential *BnaAATs* expression under the condition of cadmium-free and cadmium treatments.

Supplementary Files

This is a list of supplementary files associated with this preprint. Click to download.

- [Additionalfile1TableS1.xlsx](#)
- [FigureS1.pdf](#)
- [FigureS2.pdf](#)
- [FigureS3.pdf](#)
- [FigureS4.pdf](#)
- [FigureS5.pdf](#)
- [FigureS6.pdf](#)
- [FigureS7.pdf](#)
- [FigureS8.pdf](#)
- [FigureS9.pdf](#)
- [SupportingInformationLegends.docx](#)